ANALYSIS OF FLOW MALDISTRIBUTION IN TUBULAR HEAT EXCHANGERS BY FLUENT

A THESIS SUBMITTED IN PARTIAL FULFILLMENT OF THE

REQUIREMENTS FOR THE DEGREE OF

Master of Technology

In

Mechanical Engineering

By

K. Sudhakara Rao

Department of Mechanical Engineering

National Institute of Technology

Rourkela

2007

ANALYSIS OF FLOW MALDISTRIBUTION IN TUBULAR HEAT EXCHANGERS BY FLUENT

A THESIS SUBMITTED IN PARTIAL FULFILLMENT OF THE

REQUIREMENTS FOR THE DEGREE OF

Master of Technology

In

Mechanical Engineering

By

K.Sudhakara Rao

Under the Guidance of

Prof. R.K.Sahoo

Department of Mechanical Engineering

National Institute of Technology

Rourkela

2007

National Institute of Technology
Rourkela

CERTIFICATE

This is to certify that the thesis entitled "ANALYSIS OF FLOW MALDISTRIBUTION IN TUBULAR HEAT EXCHANGERS BY FLUENT" submitted by Sri K. Sudhakara Rao in partial fulfillment of the requirements for the award of Master of Technology Degree in Mechanical Engineering with specialization in Thermal Engineering at the National Institute of Technology, Rourkela (Deemed University) is an authentic work carried out by him under my supervision and guidance.

To the best of my knowledge, the matter embodied in the thesis has not been submitted to any other University / Institute for the award of any Degree or Diploma.

Date

Prof. R.K.Sahoo
Dept. of Mechanical Engg.
National Institute of Technology
Rourkela-769008

CONTENTS

ACKNOWLEDGEMENT

I am extremely fortunate to be involved in an exciting and challenging research project like analysis of heat exchangers. It has enriched my life, giving me an opportunity to look at the origin of technology with a wide view and to come in contact with people endowed with many superior qualities.

I would like to express my deep sense of gratitude and respect to my supervisor Prof. Ranjit Kumar Sahoo, for his excellent guidance, suggestions. He has not only been a wonderful supervisor but also a genuine person. I consider myself extremely lucky to be able to work under guidance of such a dynamic personality. Actually he is one of such genuine person for whom my words will not be enough to express.

I would like to extend my sincere thanks to Dr.A.K. Satapathy for his constant support and encouragement to perform the project work and giving us 24 hours lab facility. I am very much thankful to him for giving his valuable time for us.

I would like to express my thanks to Er.Y.P.Banjare for his encouragement.Thanks to all my bathmats in mechanical engineering department and many of friends in Hall of residence 6 for making my stay in N.I.T. Rourkela a pleasant and memorable experience.

I want to convey my heartiest gratitude to my parents and my brother for their unfathomable encouragement. The sacrifice they made to make my dream come true beyond any words I can write.

ABSTRACT

One of the common assumptions in basic design theory is that fluid be distributed uniformly at the inlet of the exchanger on each side fluid side and through out the core. However, in practice, flow maldistribution is more common and significantly reduces the desired heat exchanger performance. Maldistribution is the nonuniform distribution of mass flow rate on one or both fluid sides in the heat exchanger core. The major feature of gross flow maldistribution is that non uniform flow occurs at the macroscopic level due to poor header design or blockage of some flow passages during manufacturing, including brazing or operation. Maldistribution causes a significant increase in heat exchanger pressure drop and some reduction in heat transfer rate.

In this study, the commercial computational fluid dynamic (CFD) package, Fluent was utilized for modeling the tubular single pass heat exchanger with different tube arrangements namely four tube in-line arrangement, two tube in-line arrangement and square pitch tube arrangement. In each arrangement both flow maldistribution and uniform mass flow distribution are considered. In heat transfer terminology there appear two mean temperatures namely cross-sectional mean temperature and adiabatic mean temperature. The cross-sectional temperature is the arithmetic mean of all tube side temperatures and the adiabatic mean temperature is weighted mean of tube side temperatures.

The purpose of this investigation is to study the cross sectional mean temperature and adiabatic mean temperature profiles in the computational domain, tubular single pass heat exchanger for flow maldistribution or uniform mass flow distribution on tube side and ideal plug flow on shell side.

It is investigated that for uniform mass flow distribution on tube side and ideal plug flow on shell side, there is no difference the cross-sectional mean temperature and adiabatic mean temperature. But for maldistribution with out back flow on tube side and ideal plug flow on shell side, the two mean temperatures have same value at the cross-section $\xi=0$. For maldistribution with back flow on tube side and ideal plug flow on shell side, the temperature jump occurs at the beginning of the calculation domain.

A large computational effort is involved for the memory access of the computers and computing time for the simulation of the complex geometries associated with the dense grids. The available computational fluid dynamics software package FLUENT is applied to determine the related problems. Standard k - ε turbulence model is allowed to predict the three-dimensional flow and the conjugate heat transfer characteristics.

List of figures

List of Tables

NOMENCLATURE

Symbol	definition
A	heat transfer area, m2
j	counter of channels
k	overall heat transfer coefficient, W m2/K
L	nominal length of heat exchanger, m
N	number of tubes
NTU	number of transfer units, NTU= $kA/\dot{W}$, dimensionless
T	temperature, K
ΔT	temperature difference, K
ΔTm	cross-sectional mean temperature difference, K
ΔTad	adiabatic mean temperature difference, K
S	total set of tubes (j=1, N)
SI	subset of S with forward flow
SII	subset of S with backward flow
$\dot{W}$	thermal flow rate, W/K
w	flow velocity, m/s
$\overline{W}$	mean flow velocity, m/s
x	space coordinate, m
ε	dissipation rate of turbulent kinetic energy
κ	von Karman constant
ρ	density
$\rho\overline{u'_j u'_i}$	Reynolds stresses
μ	viscosity
σ_ε	turbulent prandtl numbers for ε
σ_k	turbulent prandtl numbers for k

μ_t	turbulent or eddy viscosity
τ_w	wall shear stresses
C_μ	dimension less constant
$C_{1\varepsilon}$	k- ε turbulence model constants
C_2	inertial resistance factor
$C_{2\varepsilon}$	k- ε turbulence model constants
C_{ij}	prescribed matrix
K	thermal conductivity, turbulent kinetic energy
P	pressure
p'	pressure correction
t	time
T	Temperature, Time averaging interval
$\overline{u_t}$	mean velocity parallel to the wall
u_τ	shear velocity
u,v,w	velocity
u', v', w'	velocity corrections
u_j	velocity in jth direction
x_i	spatial co ordinate in the ith direction

Greek symbols

θ	dimensionless temperature, $\theta = (T - T_2')/(T_1' - T_2')$
ξ	dimesionless spatial variable $\xi = \frac{x}{L}$

Subscripts

1	fluid 1
2	fluid 2
back	backward flow in tubes
f	adiabatic mean
forward	forward flow in tubes
m	cross-sectional mean

Superscripts

‘	inlet
+	at the boundary with higher value of ξ
-	at the boundary with lower value of ξ

Chapter 1

INTRODUCTION

1.1 INTRODUCTION

One of the important processes in engineering is the heat exchange between flowing fluids, and many types of heat exchangers are employed in various types of installations, as petrol-chemical plants, process industries, pressurized water reactor power plants, nuclear power stations, building heating, ventilating, and air-conditioning and refrigeration systems. As far as construction design is concerned, the tubular or shell and tube type heat exchangers are widely in use.

The shell-and-tube heat exchangers are still the most common type in use. They have larger heat transfer surface area-to-volume ratios than the most of common types of heat exchangers, and they are manufactured easily for a large variety of sizes and flow configurations. They can operate at high pressures, and their construction facilitates disassembly for periodic maintenance and cleaning. The shell-and-tube heat exchangers consist of a bundle of tubes enclosed within a cylindrical shell. One fluid flows through the tubes and a second fluid flows within the space between the tubes and the shell. Typical Shell-and-Tube heat exchanger is shown in Figure 1.1.
Heat exchangers in general and tubular heat exchangers in particular undergo deterioration in performance due to flow maldistribution. The common idealization in the basic tubular heat exchanger design theory is that the fluid is distributed uniformly at the inlet of the exchanger on each fluid side throughout the core. However, in practice, flow maldistribution is more common and significantly reduces the idealized heat exchanger performance. Flow maldistribution can be induced by the heat exchanger geometry, operating conditions (such as viscosity or density-induced maldistribution), multiphase flow, fouling phenomena, etc. Geometry-induced flow maldistribution can be classified into gross flow maldistribution, passage-to-passage flow maldistribution and manifold-induced flow maldistribution.

The flows in shell-and-tube heat exchangers have only been investigated analytically [1,2, and 3] due to their complexity. Ranjit Kumar Sahoo , Wilfried Roetzel [2] and Chakkrit Na Ranong[1] carried out an analysis of the effect of maldistribution on the thermal performance and the temperature distribution in shell and tube heat exchanger using a finite difference method.

Mueller and Chiou [17] summerised various types of flow maldistribution in heat exchangers and discussed the reason leading to flow maldistibution. . Ranganayakulu and Seetharamu [19] carried out an analysis of the effects of inlet fluid flow nonuniformity on the thermal

performance and pressure drop in crossflow plate-fin heat exchangers by using a finite element method. Lalot and Florent [4] used the computer code STAR-CD to study the gross flow maldistribution in an electrical heater. They found that reverse flows would occur for the poor header design and the perforated grid can improve the fluid flow distribution. However, few authors studied the fluid flow maldistribution using the computational fluid dynamics (CFD) simulation technique, especially the effects of the configuration of header and distributor on the flow distribution in plate-fin heat exchangers. CFD simulation technique can provide the flexibility to construct computational models that are easily adapted to a wide variety of physical conditions without constructing a large-scale prototype or expensive test rigs. Therefore, CFD can provide an effective platform where various design options can be tested and an optimal design can be determined at a relatively low cost.

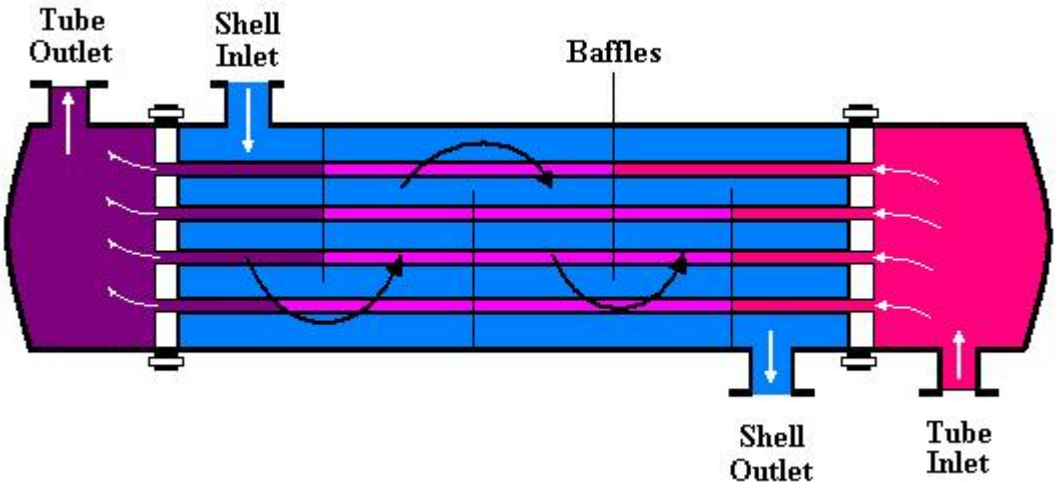

Fig 1.1 Shell-and-tube heat exchanger

A heat exchanger is a device built for efficient heat transfer from fluid one to another, whether the fluids are separated by a solid wall so that they never mix, or the fluids are directly contacted. They are widely used in petroleum refineries, chemical plants, petrochemical plants, natural gas

processing, refrigeration, power plants, air conditioning and space heating. One common example of a heat exchanger is the radiator in a car, in which a hot engine-cooling fluid, like antifreeze, transfers heat to air flowing through the radiator.

1.2 Classification of heat exchangers

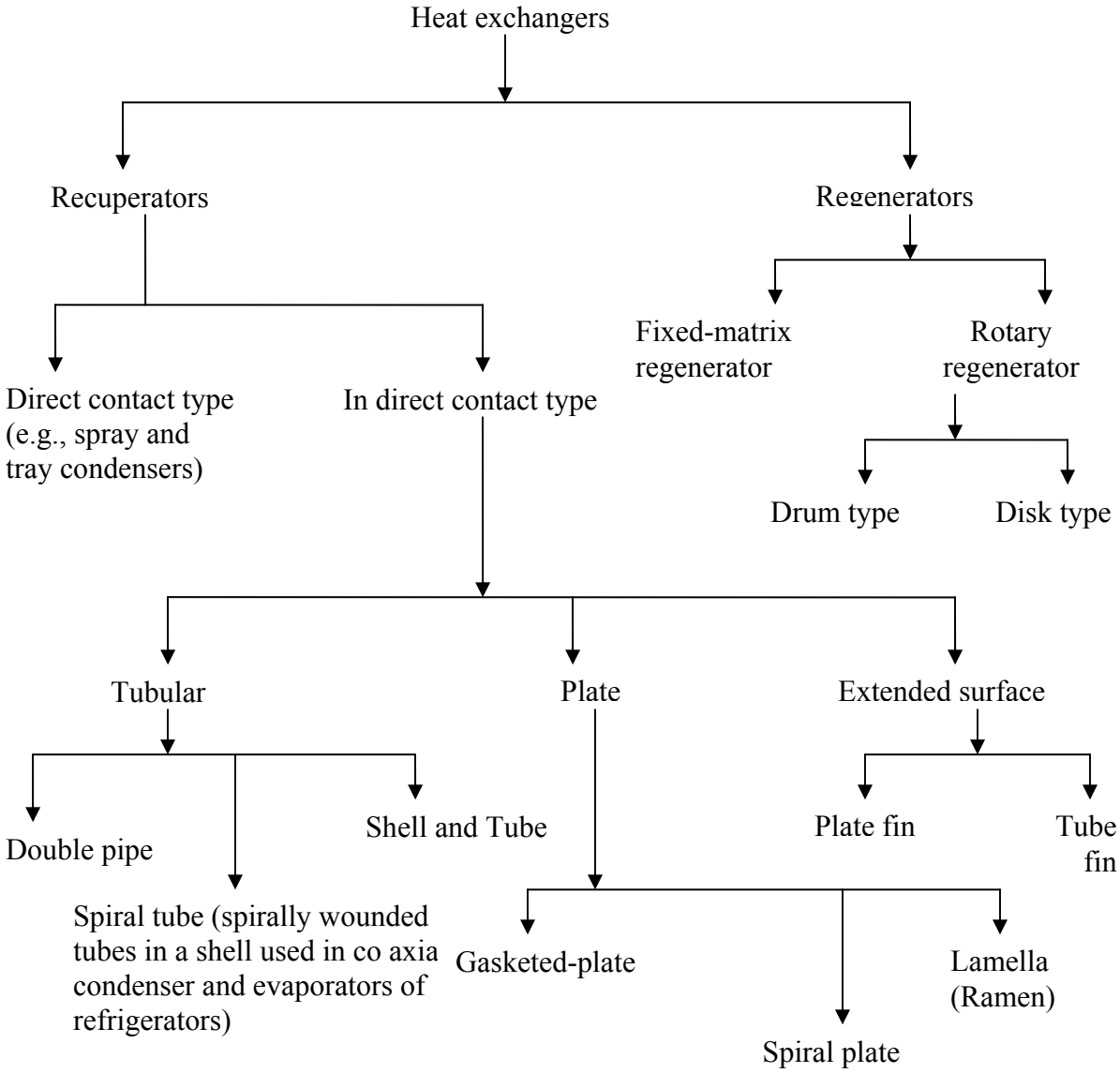

1.3 Tubular heat exchangers

Tubular heat exchangers are generally built of circular tubes, although elliptical, rectangular or round/flat twisted tubes have also been used in some applications. There is considerable flexibility in design because the core geometry can be varied easily by changing the tube diameter, length, and arrangement. Tubular exchangers can be designed for high pressures relative to environment and high-pressure differences between the fluids. Tubular exchangers are used primarily for liquid-to-liquid and liquid to phase change (condensing or evaporating) heat transfer applications. There are used for gas-to liquid and gas-to-gas heat transfer applications primarily when the operating temperature and /or pressure is very high or fouling is a severe problem on at least one fluid side and no other types of exchangers work.

These tubular exchangers may be classified as shell-and-tube, double-pipe, and spiral tube exchangers. There are all prime surface exchangers except for exchangers having fins out side/inside tubes.

1.3.1 Double pipe heat exchanger:

A typical double-pipe heat exchanger consists of one pipe placed concentrically in side another of larger diameter with appropriate fittings to direct the flow from one section to the next, as shown in figure (1.2). Double-pipe heat exchangers can be arranged in various series and parallel arrangements to meet pressure drop and mean temperature difference requirements. The major use of double-pipes exchangers is for sensible heating or cooling of process fluids where small heat transfer areas (to 50 $m^{2)}$ are required. This configuration is also very suitable. When one or both fluids is at high pressure. The major disadvantage is that double-pipe heat exchangers are bulky and expensive per unit transfer surface. Inner tube being may be single tube or multi-tubes Fig. (1.3). If heat transfer coefficient is poor in annulus, axially finned inner tube (or tubes) can be used. Double-pipe heat exchangers are built in modular concept, i.e., in the form of hair fins.

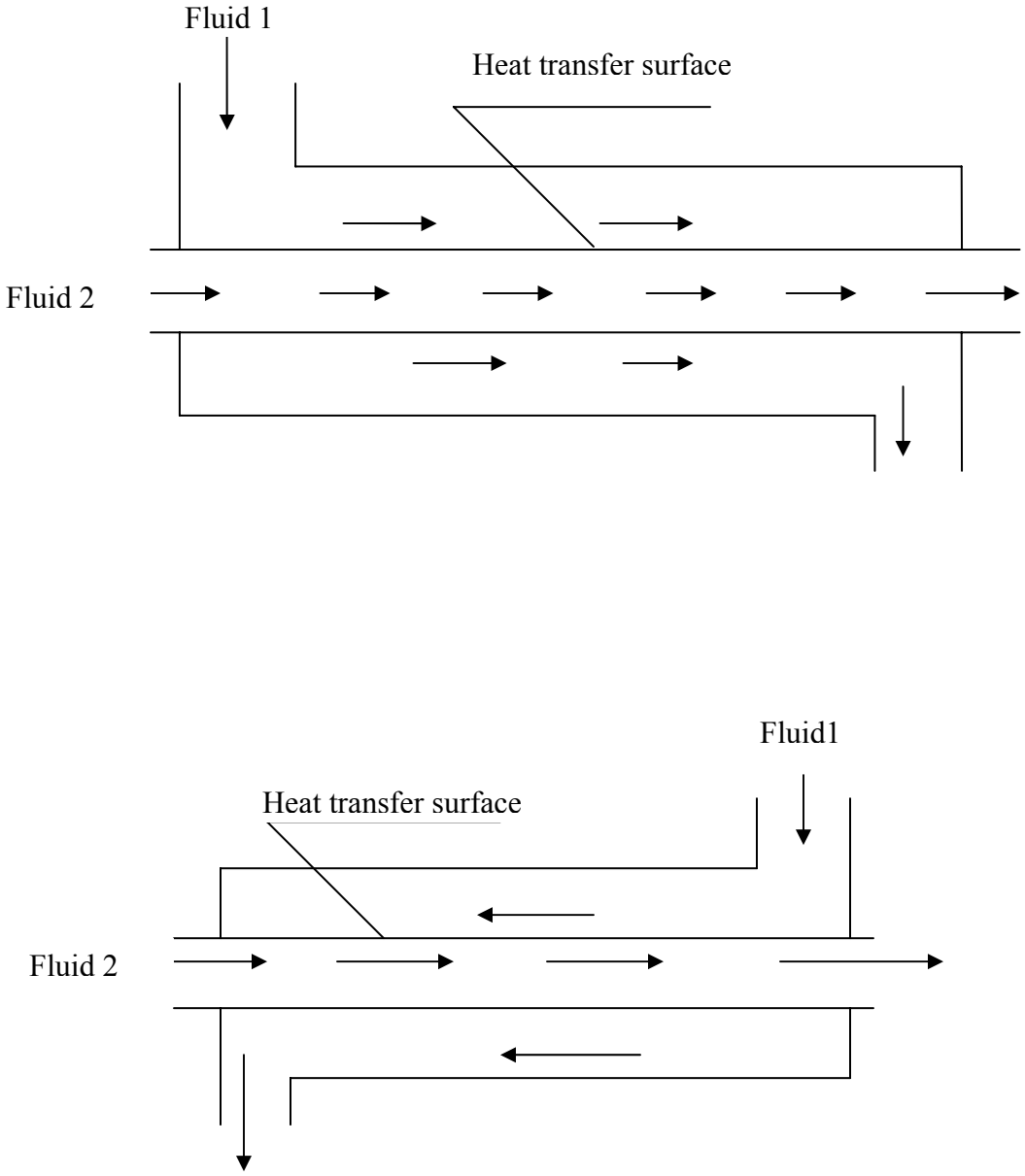

Fig 1.2: Double pipe heat exchanger

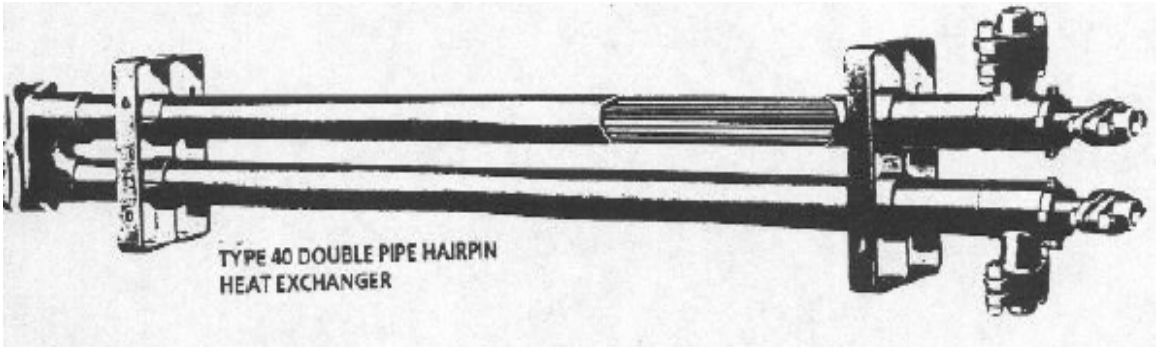

Fig 1.3: Double pipe hair-pin heat exchanger with cross sectional view and return bend housing

1.3.2 Shell-and-tube Heat exchanger:

Shell-and-tube heat exchangers are built of round tubes mounted in large cylindrical shells with the tube axis parallel to that of the shell. These are commonly used as oil coolers, power condensers, preheaters and steam generators in both fossil fuel and nuclear-based energy production applications. They are also widely used in process applications and in the air conditioning and refrigeration industry. Although they are not specially compact, their robustness and shape make them well suited for high pressure operations. They have larger heat transfer surface area-to-volume ratios than the most of common types of heat exchangers, and they are manufactured easily for a large variety of sizes and flow configurations. They can operate at high pressures, and their construction facilitates disassembly for periodic maintenance and cleaning. The shell-and-tube heat exchangers consist of a bundle of tubes enclosed within a cylindrical shell. One fluid flows through the tubes and a second fluid flows within the space between the tubes and the shell. The simplest form of a horizontal shell-and-tube type condenser with various components is shown in fig (1.4). One fluid flows on the shell-side steam flows across between pair of baffles and then flows parallel to the tubes as it flows from one baffle compartment to the next. There are wide differences between shell-and-tube heat exchangers

depending on the application. The most representative tube bundle types used in shell-and-tube heat exchangers are shown in figures,

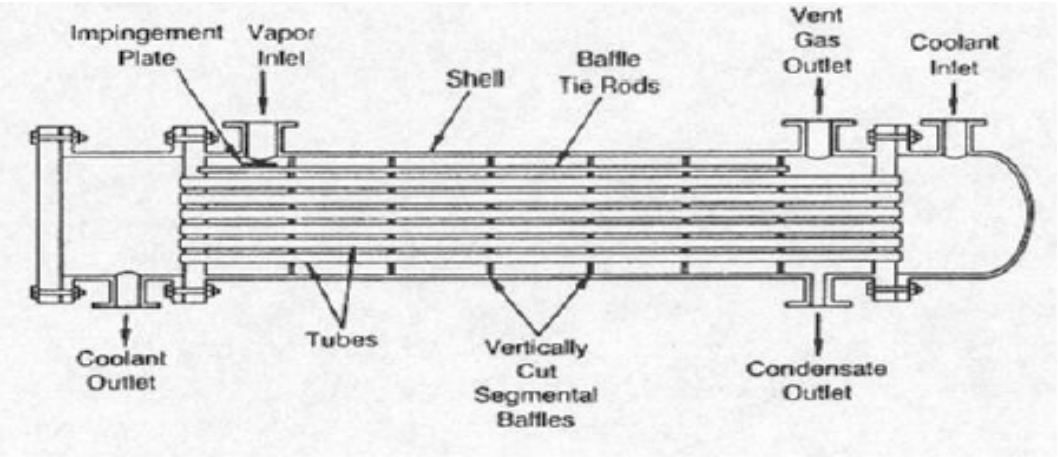

Fig 1.4: Shell-and-tube heat exchanger as a shell-side condenser: TEMA E-type shell with single tube side

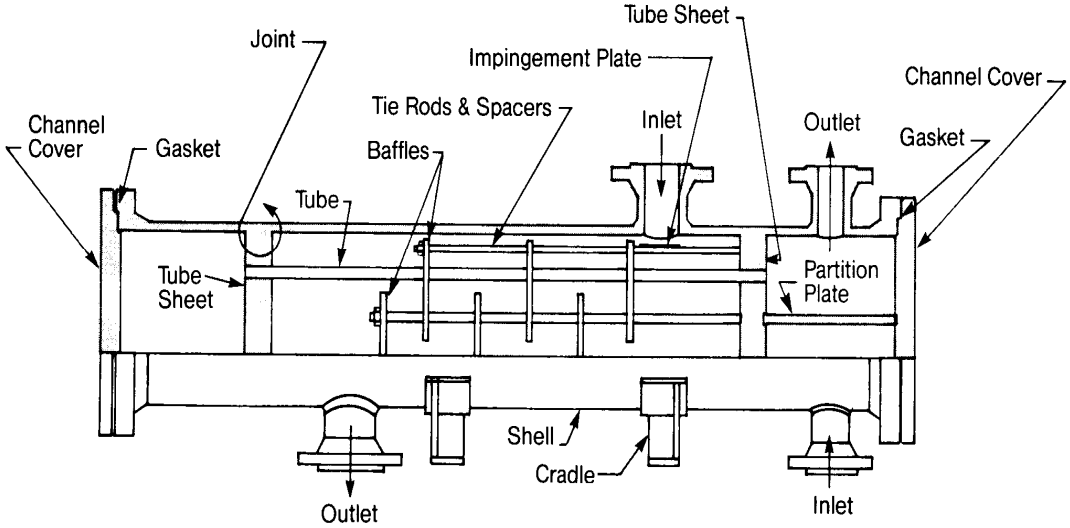

A

Fixed Tube sheet Heat exchanger

Fig 1.5: Two-pass tube, baffled single-pass shell, shell-and-tube heat exchanger.

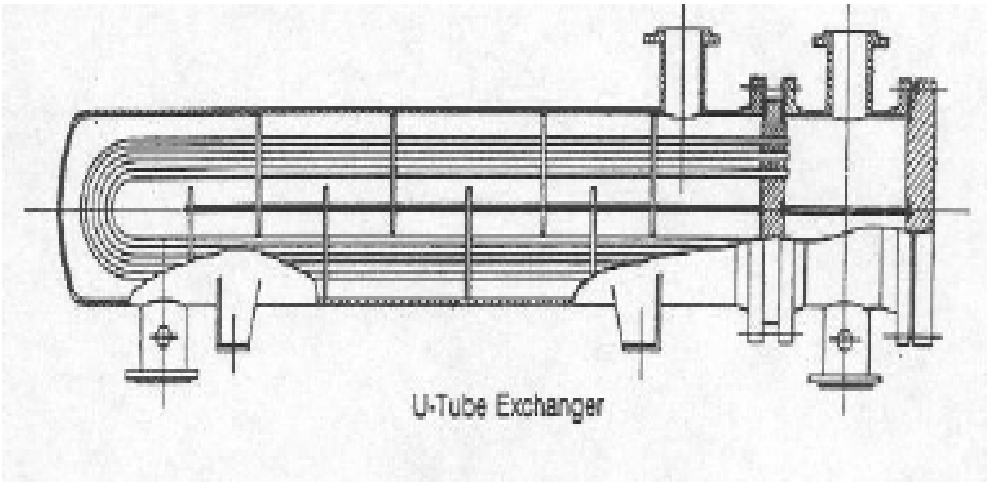

Fig 1.6: A U-tube, baffled single-pass shell, shell-and-tube heat exchanger.

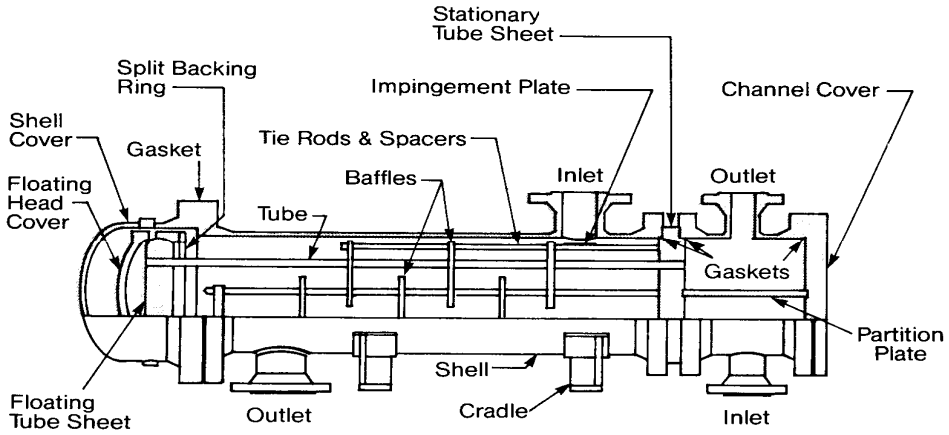

Fig 1.7: Pull-Through Floating-Head Heat Exchanger

1.3.3 Spiral tube heat exchangers:

Spiral-tube heat exchangers consist of one or more spirally wound coils fitted in a shell or designed as co axial condensers and co-axial evaporators that are used in refrigeration systems.

Heat transfer rate associated with a spiral tube is higher than that for a straight tube. In addition, a considerable amount of surface can be accommodated in a given space by spiraling. Thermal expansion is no problem, but cleaning is almost impossible.

A spiral tube heat exchanger is a coil assembly fitted in a compact shell that optimizes heat transfer efficiency and space. Every Sentry spiral coil assembly has welded tube to manifold joints and uses stainless steel as a minimum material requirement for durability and strength. The coil assembly is welded to a head and fitted in a compact shell. The spaces or gaps between the coils of the spiral tube bundle become the shell side flow path when the bundle is placed in the shell. Tube side and shell side connections on the bottom or top of the assembly allow for different flow path configurations. The spiral shape of the flow for the tubeside and shellside fluids creates centrifugal force and secondary circulating flow that enhances the heat transfer on both sides in a true counter flow arrangement. You get the advantage of tube side enhancement without the associated potential for plugging on both the shell and tube side of the heat exchanger. Since there are no baffles or dead spots to lower velocities and coefficients, heat transfer performance is optimized. Additionally, since there are a variety of multiple parallel tube configurations (diameter, number and length), efficiency is not compromised by limited shell diameter sizes as it is in shell and tube designs. The profile of a spiral is very compact and fits in a smaller footprint than a shell and tube design. Since the tube bundle is coiled, space requirements for tube bundle removal are virtually eliminated. When exotic material is required, a spiral tube heat exchanger minimizes the material used since manifolds replace the channels, heads and tube sheets of a conventional shell and tube design.

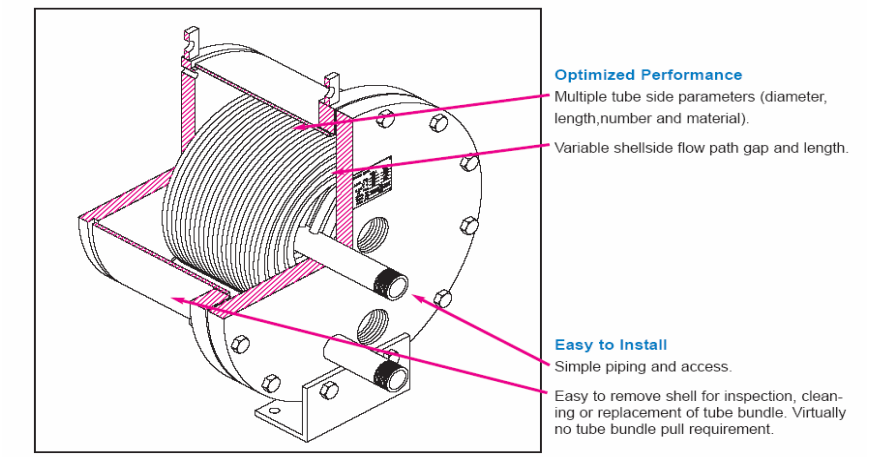

Fig 1.8 Cross-section of Spiral Tube heat exchanger

1.4 Objectives of the work

The objective of the present study is to provide more complete understanding Flow maldistribution in tubular heat exchanger by studying area weighted and mass weighted temperature profiles for maldistribution with out back flow and maldistribution with back flow. And comparison of average temperature profiles of flow maldistribution with the average temperature profiles of uniform mass flow distribution.

This numerical investigation was carried out for the in-line tube arrangement with different number of tubes. A finite volume numerical scheme is used to predict the conjugate heat transfer and fluid flow characteristics with the aid of the computational fluid dynamics (CFD) commercial code, FLUENT. The governing equations for the energy and momentum conservation were solved numerically with the assumption of three-dimensional steady flow. An effective model, the standard based k-ε turbulence model was applied in this investigation.

As described in the section 2.2, the available relevant literature is quite limited With respect to the analytical and it is still difficult to predict the physics of the flow maldistribution within the circular tube banks. Therefore, temperature distributions with in the bundle were studied numerically.

Chapter 2

LITERATURE REVIEW

2.1. Introduction

The literature reviewed in this chapter can be broadly classified under three categories.

The first part of the survey deals with the analytical solution for maldistribution in shell and tube heat exchanger. Second part of the survey deals with the experimental and CFD analysis of maldistribution in heat exchanger, and third part of the survey deals with the analysis of maldistribution in plate heat exchanger.

2.2. Analysis of maldistribution in shell and tube heat exchanger by analytical method

Wilfried Roetzel, Chakkrit Na Ranong., [1] calculated the axial temperature profiles in a shell and tube heat exchanger by numerically for given maldistributions on the tube side. For comparison the same maldistributions are handled with the parabolic and hyperbolic dispersion model with fitted values for the axial dispersion coefficient and third sound wave velocity. The analytical results clearly demonstrate that the hyperbolic model is better suited to describe the steady state axial temperature profiles. For a global consideration of a heat exchanger with maldistribution the parabolic model is satisfactory. The parameter Pepar depends on the NTU of the maldisributed flow stream and on the NTU of the transversely mixed flow stream which makes the model difficult to handle. The hyperbolic model predicts the axial temperature profiles correctly, especially temperature jumps and positive slopes. The third sound Mach number M characterizes the type of flow maldistribution and is independent of both NTUs. For a given type of relative flow maldistribution Pehyp is proportional to the NTU of the maldistributed flow stream but does not depend on the other NTU:

Sahoo, R.K., and Wilfried Roetzel., [2] derived The fundamental equations of hyperbolic model and its boundary conditions in terms of cross-sectional mean temperature from the basic equations of heat exchanger The traditional parabolic model and the proposed hyperbolic model which includes the parabolic model as a special case can be used for dispersive flux formulation. Instead of using the heuristic approach of parabolic or hyperbolic formulation, these models can

be quantitatively derived from the axial temperature profiles of heat exchangers. In this paper both the models are derived for a shell-and-tube heat exchanger with pure maldistribution (without back mixing) in tube side flow and the plug flow on the shell side. The Mach number and the boundary condition which plays a key role in the hyperbolic dispersion have been derived and compared with previous investigation. It is observed that the hyperbolic model is the best suited one as it compares well with the actual calculations. This establishes the hyperbolic model and its boundary conditions.

Wilfried Roetzel, and Chakkrit Na Ranong.,[3] tested and compared the newer hyperbolic dispersion model and parabolic model considering the processes with pure maldistribution (with out back mixing) on the tube side of a shell and tube heat exchanger and plug flow on shell side . The boundary conditions of the model equations are discussed in detail for the steady state and equations of the axial temperature profiles are provided in the programmable form. For the hyperbolic model simple relationships between the model parameters are derived. Considering the transient adiabatic processes in the tube bundle a concept for the experimental determination of the model parameter M, the third sound Mach number, is developed. Authors concluded that for an overall consideration of a heat exchanger with maldistribution the parabolic model is satisfactory. The parameter Pe_{par} depend on both NTUs of the heat exchanger which makes the model difficult to handle. The advantage of the parabolic model is that only the only one parameter is needed. The hyperbolic model is superior to the parabolic model because it predicts the axial temperature profiles correctly, especially temperature jumps and (positive) slopes.

Yimin xuan, wilfried roetzel, [4] Applied the dispersion model is to the description of the effects of shell and tube side flow maldistribution. By means of this model, an efficient and versatile method of predicting transient response of multi pass shell and tube heat exchangers is developed. The method allows for effect of maldistribution on transient process, influence of heat capacities of fluids and solid components, arbitrary inlet temperature variations and step disturbances of flow rates. General forms of initial conditions and two different flow arrangements are considered. A general form of the solution for steady-state and dynamic simulation is derived. Temperature profiles are determined with numerical inversion of the Laplace transform. Some examples are calculated and the effect of maldistribution is discussed. Flow maldistribution hinders transient responses to any inlet changes and decreases thermal effectiveness of heat exchangers. Its effect becomes more remarkable with increasing NTC'. The

Peclet number has been used to quantitatively describe this kind of effect. The calculation has shown that the dispersion model should be applied instead of the plug-flow model if Pe < 55.

Danckwerts, p. v., [5]
When a fluid flows through a vessel at a constant rate, either “piston-flow” or perfect mixing is usually assumed. In practice many systems do not conform to either of these assumptions, so that calculations based on them may be in accurate. It is explained how distribution functions for residence-times can be defined and measured for actual systems. Open and packed tubes are discussed as systems about which predictions can be made. . The use of the distribution functions is illustrated by showing how they can be used to calculate the efficiencies of reactors and blenders. It is shown how models may be used to predict the distribution of residence-times in large systems.

2.3. Experimental and CFD analysis of flow maldistribution in heat exchanger:

Lalot, S., Florent, p., Langc, S.K., and Bergles, A.E., [6] experimentally observed the gross-flow maldistribution in an electrical heater the effect of flow nonuniformity on the performance of heat exchangers. First, it is shown that it is much more important to understand maldistributions for electrical heaters than for two fluid heat exchangers. The study of the flow distribution in a particular heater shows that reverse flows may occur for poor inlet header design. Suggested here is a simple way to homogenize the flow distribution and a simple law to calculate, with good accuracy, the velocity ratio (ratio of the highest velocity in the tubes to the lowest velocity). The original fluid distribution is applied to heat exchangers (condensers, counter flow and cross flow heat exchangers), and it is shown that gross flow maldistribution leads to a loss of effectiveness of about 7% for condensers and counter flow heat exchangers, and up to 25% for cross flow exchangers, for velocity ratios up to 15.

Prabhakara Rao Bobbili., Bengt Sunden., and Sarit Kumar Das., [7] carried out experiments to find the flow and the pressure difference across the port to channel in plate heat exchangers for a wide range of Reynolds number, 1000–17000. In the present study, low corrugation angle plates

have been used for different number of channels, namely, 20 and 80. Water has been used as working fluid for both hot and cold fluids. The pressure probes are inserted through the plate gasket into both the inlet and exit ports of the channel. The pressure drop is recorded at the first, middle and last channels for each plate package of the heat exchanger. Also, the overall pressure drop has been measured for various flow rates. This overall pressure drop is a function of the flow rate, the cross-sectional area ratio of channel to port and number of channels per fluid. A simplified non-dimensional channel velocity has been suggested based on the channel pressure drop and the mean channel pressure drop of plate package, to measure the deviation of the particular channel flow rate from the mean channel flow rate. The results indicated that the flow maldistribution increases with increasing overall pressure drop in the plate heat exchangers.

Žarko Stevanović., Gradimir Ilić., Nenad Radojković., Mića Vukić2, Velimir Stefanović2, Goran Vučković2,.[8] described , a numerical study of three-dimensional fluid flow and heat transfer in a shell and tube model heat exchanger. An iterative procedure for sizing shell-and-tube heat exchangers according to prescribed pressure drop is shown, then the thermo-hydraulic calculation and the geometric optimization for shell and tube heat exchangers on the basis of CFD technique have been carried out. Modeling of shell and tube heat exchangers for design and performance evaluation is now an established technique used in industry. . The baffle and tube bundle was modeled by the 'porous media' concept. Three turbulent models were used for the flow processes. The velocity and temperature distributions as well as the total heat transfer rate were calculated. The calculations were carried out using PHOENICS Version 3.3 code. The effect of different turbulence models on both flow and heat transfer is significant. This is due to the introduction effects of eddy-viscosity. It was concluded that Chen-Kim modification of the standard k-ε turbulence model give the best agreement to the experimental data of velocity field.

2.4. Analysis of maldistribution in plate heat exchanger by analytical method

Wilfried Roetzel and SARIT K.DAS., [9] Introduced **a** new concept of hyperbolic axial dispersion in fluid. This is an extension of the already established method of considering axial dispersion which takes the flow maldistribution into account in the analysis of heat exchangers. The concept is introduced by analogical treatment of the axial dispersion with the fluid conduction. Hyperbolic conduction, which considers a finite conduction wave propagation

velocity, is important only in special cases such as cryogenic temperatures or sudden incidence of high heat flux. On the other hand the similar propagation velocity of the dispersion wave appears to be a general phenomenon which affects the thermal performance of heat exchangers even for common applications. Based on the proposed theoretical foundation, the dynamic analysis of a U-type plate heat exchanger is presented for step and sinusoidal change in one of the inlet temperatures. For this purpose the traditional inlet boundary condition for the dispersion model has been extended to incorporate the effect of the finite propagation velocity of the dispersion wave. The method of Laplace transforms has been applied for the analysis, and the Laplace inversion is carried out numerically using fast Fourier transforms. The results indicate that the proposed concept of 'hyperbolic dispersion' can be developed as a powerful tool for the analysis of heat exchangers particularly in the transient regime of operation.

Anindya Roy, and Sarit K. Das., [10] utilized a modern technique based on the “axial dispersion model” has been to simulate the regenerative heat exchanger both in the warm-up and pseudo-steady state operation. The advantage of this model is that it takes all the flow maldistribution and backmixing effects into consideration instead of idealizing the flow to be so called “plug flow”. In contrast to previous studies with dispersion, in the present study the dispersion is considered to propagate with a finite propagation velocity following a hyperbolic law which is physically more consistent. The effect of different parameters on the cyclic response has been brought out and the results have been verified by comparing results of a rotary regenerator. The technique utilized in the present study can act as a tool for modelling regenerators where non-uniformity in flow distribution is significant.

Ping Yuan., [11] investigates the effect of flow maldistribution on the thermal performance of a three-fluid crossflow heat exchanger by the numerical method. In the inlets of three fluid streams, this study considers four modes of flow nonuniformity arrangement by using three flow maldistribution models. According to the results of temperature fields, effectiveness and deterioration factor, this study discusses the deterioration or promotion due to the flow maldistribution in the heat exchanger. The results indicate that there is a best one in choice between the four maldistribution modes and the best flow maldistribution mode promotes the thermal performance of a three-fluid crossflow heat exchanger when NTU and heat capacity rate ratios are large.

Srihari, N., and, Prabhakara Rao, B., Bengt Sunden, Sarit and K. Das., [12] analysis represents the dynamic behavior of the single pass plate heat exchangers, considering flow maldistribution from port to channel. In addition to maldistribution the fluid axial dispersion is used to characterize the back mixing and other deviations from plug flow. Due to unequal distribution of the fluid, the velocity of the fluid varies from channel to channel and hence the heat transfer coefficient variation is also taken into consideration. Solutions to the governing equations have been obtained using the method of Laplace transform followed by numerical inversion from frequency domain. The results are presented on the effects of flow maldistribution and conventional heat exchanger parameters on the temperature transients of both U-type and Z-type configurations. It is found that the effect of flow maldistribution is significant and it deteriorates the thermal performance as well as the characteristic features of the dynamic response of the heat exchanger. In contrast to the previous studies, here the axial dispersion describes the in channel back mixing alone, not maldistribution, which is physically more appropriate. Present method is an efficient and consistent way of describing maldistribution and back mixing effects on the transient response of plate heat exchangers using an analytical method without performing intensive computation by complete numerical simulation.

Roetzel, W., Spang, B., Luo, X., and Dash, S.K., [13] Proposed the emerging concept of dispersion of heat along the axial direction as a fluid flows through a passage bounded by solid wall has been presented with its most recent and remarkable advancement. This new proposition takes axial dispersion as a disturbance which propagates as a wave with a finite velocity. It has been proposed that this sound like propagation be named as the “third sound wave in flowing fluid”. The fundamental analysis of this theory has been presented with particular emphasis on the boundary condition which plays a key role in the propagation of the wave. A general flux formulation has been used for this purpose. Analysis has also been presented for a two fluid situation. It has been found that the ‘subsonic’ and ‘super sonic’ flow with respect to third sound wave behave differently particularly at entry and exit. The theoretical background developed has been substantiated by three examples-one purely theoretical condition, one comparison with numerical analysis and finally application to a complete apparatus.

Zhe Zhang and YanZhong Li., [14] Used a computational fluid dynamics (CFD) program FLUENT has been used to predict the fluid flow distribution in plate-fin heat exchangers. It is

found that the flow maldistribution is very serious in the *y* direction of header for the conventional header used in industry. The results of flow maldistribution are presented for a plate-fin heat exchanger, which is simulated according to the configuration of the plate-fin heat exchanger currently used in industry. The numerical prediction shows a good agreement with experimental measurement. By the investigation, two modified headers with a two-stage-distributing structure are proposed and simulated in this paper. The numerical investigation of the effects of the inlet equivalent diameters for the two-stage structures has been conducted and also compared with experimental measurement. It is verified that the fluid flow distribution in plate-fin heat exchangers is more uniform if the ratios of outlet and inlet equivalent diameters for both headers are equal.

Xuan, Y., and Roetzel, W., [15] Developed a versatile and efficient method is developed for predicting dynamic performances of parallel and counterflow heat exchangers subject to arbitrary temperature variations and step flow disturbances, including the effect of flow maldistribution and the influence of heat capacities of both fluids, shell wall and tube bank as well as nonzero initial temperatures. Two algorithms of numerical inversion of the Laplace transform are introduced to determine the final temperature profiles in the realtime domain and some examples are calculated with nonuniform initial conditions. The accuracy of the proposed method is demonstrated with the calculated results at new steady states. Experiments are carried out on a labor-sized heat exchanger to further examine the feasibility of this method and the comparison between calculated and measured temperature profiles is illustrated and discussed.

Wilfried Roetzel and Frank Balzereit., [16] The effect of the deviation of the actual three-dimensional flow field on the shell-side from the frequently assumed one-dimensional uniform axial plug flow can be taken into account by superimposed axial dispersion in the fluid. The measure for axial dispersion is the Peclet number which can vary from infinite (no dispersion) to zero (complete axial mixing). For the fast and more reliable calculation of transient processes with the axial dispersion model, the Péclet number has to be known. A residence time distribution measurement technique for the determination of shell-side dispersive Peclet numbers is described and used to determine Peclet numbers for different shell-to-baffle clearances, numbers of baffles, and axial plug flow Reynolds numbers. Measurements with water reveal that Peclet numbers from 15 to 160 can occur and axial dispersion cannot be neglected in many cases.

Mueller, A.C., [17] concluded that the effects of several types and patterns of maldistribution in heat exchangers on the exchanger thermal performance are investigated. For turbulent flow most exchangers show only a small reduction in performance; however, for laminar flow the reduction can be large. It is shown that substantial errors in the apparent heat transfer coefficient occur for nonuniform flows.

Anil Kumar Dwivedi, and Sarit Kumar Das., [18**]** presented **a** predictive model suggest the transient response of plate heat exchangers, subjected to a step flow variation. The work also brings out the effect of the port to channel maldistribution on the performance of plate heat exchangers under the condition of flow variation. The results indicate that flow maldistribution affects the performance of the plate heat exchangers in the transient regime. A wide range of the parametric study has been presented which brings out the effects of NTU and heat capacity rate ratio on the response of the plate heat exchanger, subjected flow perturbation. To verify the presented theoretical model, appropriate experiments have been carried out. Experiments include the responses of the outlet temperatures subjected to inlet temperature transient in the circuit followed by a sudden change in flow rate in one of the fluids. Simulated performance has been compared to the performance measured in the experiments. Comparisons indicate that theoretical model developed for flow transient is capable of predicting the transient performance of the plate heat exchangers satisfactorily, under the given conditions of changed flow rates.

Ranganayakulu, Ch., and Seetharamu, K.N., [19] developed a mathematical equation to generate different types of fluid flow maldistribution models considering the possible deviations in fluid flow. Using these fluid flow maldistribution models, the exchanger effectiveness and its deteriorations due to the combined effects of longitudinal heat conduction and flow nonuniformity are calculated on both the cold and hot fluid sides of an exchanger for the entire range of design and operating conditions. The finite element model, introduced for the simple cross flow heat exchanger, predicts thermal performance deteriorations which are within 0.5% variation with available numerical solutions. The thermal performance deterioration of cross flow compact heat exchanger due to the combined effects LHC and FN is not always negligible, especially when the fluid capacity rate ratio of both fluids is equal to 1.0 and when the longitudinal heat conduction parameter .k. is greater than 0.005. Also, it has been observed that the performance deteriorations of cross flow heat exchanger are higher when inlet fluid flow

nonuniformity is considered. Information obtained in this study clearly indicates that the deterioration of thermal performance due to the combined effects of longitudinal heat conduction and fluid flow nonuniformity may be significant for cross flow plate-fin heat exchangers.

Karno, A., and Ajib, S., [20] prepared a new program for simulation and optimization of the shell-and-tube heat exchangers is to obtain useful results by employment of the computing technology fast and accurately. As an application of this program, the effects of transverse and longitudinal tube pitch in the in-line and staggered tube arrangements on the Nusselt numbers, heat transfer coefficients and thermal performance of the heat exchangers were investigated. The obtained values of the tube pitch were compared with literature values.

Chapter 3

FLOW MALDISTRIBUTION IN HEAT EXCHANGERS

3.1 INTRODUCTION

One of the common assumptions in basic heat exchanger theory is that fluid be distributed uniformly at the inlet of the exchanger on each fluid side and through out the core. However, in practice, flow maldistribution is more common and significantly reduces the desired heat exchanger performance. Still this influence may be negligible in many cases, and the goal of uniform flow through the exchanger is met reasonably well for performance analysis and design purposes.

Flow maldistribution is defined as of the mass flow rate on one or both sides in any of the heat exchanger ports and/or in the heat exchanger core. The term ideal fluid flow passage/header/heat exchanger would denote conditions of uniform mass flow distribution through an exchanger core.

Flow maldistribution can be induced by heat exchanger geometry (mechanical design features such as the basic geometry, manufacturing imperfections, and tolerances), and heat exchanger operating conditions (e.g., viscosity-or density-induced maldistribution, and fouling phenomena).geometry-induced flow maldistribution can be classified into (1) gross flow maldistribution, (2) passage-to-passage flow maldistribution, and (3) manifold-induced flow maldistribution. The most important flow maldistribution and associated flow instability.

3.2 GEOMETRY-INDUCED FLOW MALDISTRIBUTION

One class of flow maldistribution, which is a result of geometrically nonideal fluid flow passages or nonideal exchanger inlet/outlet header/tank/manifold/nozzle design, is referred to as geometry-induced flow maldistribution. This type maldistribution is closely related to heat exchanger construction and fabrication (e.g., header design, heat exchanger core fabrication including brazing in compact heat exchangers).this maldistribution is peculiar to a particular heat exchanger in question and can not be influenced significantly by modifying operating conditions. Geometry-induced flow maldistribution is related to mechanical design-induced flow nonuniformities such as (1) entry conditions, (2) by pass and leakage streams, (3) fabrication tolerances, (4) shallow bundle effects, and (5) general equipment and exchanger system effects.

The most important causes of flow non uniformities can be divided roughly into three main groups of maldistribution effects: gross flow maldistribution (at the inlet face of the exchanger), passage-to-passage flow maldistribution (non uniform flow in neighboring flow passages), and manifold-induced flow maldistribution (due to inlet/outlet manifold/header design).

3.2.1 Gross flow maldistribution:

The major feature of gross flow maldistribution is that nonuniform flow occurs at the macroscopic level (due to poor header design or blockage of some flow passages during manufacturing, including brazing or operation). The gross flow maldistribution does not depend on the local heat transfer surface geometry. This class of flow maldistribution may cause a significant increase in the exchanger pressure drop, and some reduction in the heat transfer rate. To predict the magnitude of these effects for some simple exchanger flow arrangements, the nonuniformity will be modeled as one-or two-dimensional as follows, with some specific results.

3.2.2 Passage-to-Passage flow maldistribution:

Compact heat exchangers with uninterrupted (continuous) flow passages, while design for nonfouling applications, are highly susceptible to passage-to-passage flow maldistribution. That is because the neighboring passages are geometrically never identical, due to imperfect manufacturing processes. It is especially difficult to control the passage size precisely when small dimensions are involved. Since differently sized and shaped passages exhibit different flow resistances and the flow seeks the path of least resistance, a nonuniform flow through the matrix results. This phenomenon usually causes a slight reduction in pressure drop, while the reduction in heat transfer rate may be significant compared to that for nominal size passages.

3.2.3 Manifold-induced flow maldistribution:

Whereas manifolds are integral in plate heat exchangers due to construction features, manifolds are common and attached separately in many other applications. In The PHEs,

The fluids enter and exit the manifolds laterally and flow with in the core axially; here the axial direction is defined as the main direction of fluid flow with in the PHE passages. In other

applications, the fluids enter and exit the core also axially, or a combination of axial lateral entry and exit. In PHEs, the manifolds are of two basic types: deviding flow and combining flow. In deviding-flow manifolds, fluids enter laterally and exits the manifold axially. The velocity with in the manifold, parallel to manifold axis, varies from the inlet velocity to zero value. Conversely, in combining-flow manifolds, fluid enters from the PHE core and exits at the end of the manifold varying from zero to the out let velocity.

3.3. Governing equations in shell-and-tube heat exchanger with maldistribution in tube side:

A shell and tube heat exchanger with pure axial plug flow on the shell side and maldistribution on the tube side shown in Fig. 3.1

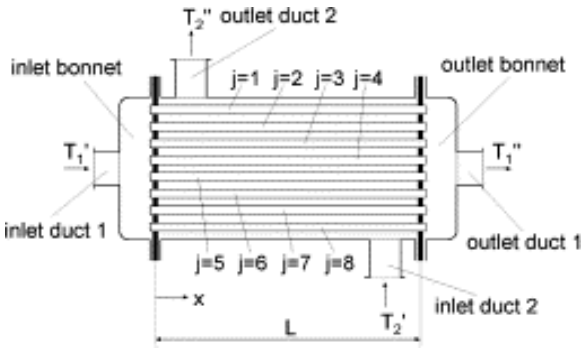

Fig.3.1. Schematic of shell-and-tube heat exchanger with tube channels (j=1,…,8).

In the shell-and-tube heat exchanger, a constant velocity of tube side fluid is usually assumed in all the tubes. Actually, the velocity may vary from tube to tube due to disadvantageous geometry of the inlet duct, outlet duct and bonnets. On the shell side, plug flow is assumed. For simplicity the overall heat transfer coef- ficient is assumed to be uniform. This type of steady state maldistribution due to flow non-uniformity in tube side gives dispersion. Under the realistic assumption of plug flow inside each of the N tubes, the tube side equation given by Ranjit Kumar Sahoo, Wilfried Roetze,l.[2] is,

$$\frac{d\theta_{1j}}{d\xi} + \frac{kA/N}{\left(\dot{W}_1/N\right)\left(W_{1J}/\overline{W_1}\right)}\left(\theta_{1J} - \theta_2\right) = 0. \tag{3.1}$$

This equation may be rewritten as

$$\frac{w_{1j}}{\overline{w_1}}\frac{d\theta_{1j}}{d\xi} + NTU_1\left(\theta_{1J} - \theta_2\right) = 0. \tag{3.2}$$

The second term of Eq. (3.2) represents the local heat flux at the jth tube due to shell side fluid. Summing up all N equations and dividing by N gives

$$\frac{1}{N}\sum_{J=1}^{N}\frac{d}{d\xi}\left(\frac{w_{1j}}{\overline{w_1}}\theta_{1j}\right) + NTU_1\left(\frac{1}{N}\sum_{J=1}^{N}\theta_{1J} - \theta_2\right) = 0, \tag{3.3}$$

Where the second term represents the average local heat flux associated with all the tube side flow and this must be equal to the lateral flux associated with the shell side fluid. Thus the shell side energy equation is given as

$$\frac{d\theta_2}{d\xi} + NTU_2\left(\frac{1}{N}\sum_{J=1}^{N}\theta_{1J} - \theta_2\right) = 0. \tag{3.4}$$

For counter flow NTU2 > 0, for cocurrent flow NTU2 < 0 and for condensation or evaporation NTU2 = 0.The mean flow velocity inside the tube bundle in the direction of ξ is always positive and can be expressed as

$$\overline{w_1} = \frac{1}{N}\sum_{J=1}^{N} w_{1j} > 0. \tag{3.5}$$

For partial back flow which is also under consideration, flow velocities in some of the tubes are negative but the mean flow velocity is always positive.

Eqs. (3.2) and (3.4) generate N + 1 equations which are to be solved by specifying the boundary conditions below.

For no back flow, the boundary conditions are given by Eqs. (3.6)– (3.8):

(i) For counter flow and cocurrent flow without back flow (w1j > 0; j = 1;N)

$$\xi = 0: \quad \theta_{1j} = \theta_1^- = 1. \tag{3.6}$$

(ii) For counter flow (NTU2 > 0)

$$\xi = 1: \quad \theta_2 = 0. \tag{3.7}$$

(iii) For cocurrent flow (NTU2 < 0)

$$\xi = 0: \theta_2 = 0. \tag{3.8}$$

In case of back flow in some of the tubes $\left(\overline{w_1} > 0\right)$, let the set of tubes SI have the forward flow and the set SII have the backward flow. Thus, $S_I \subset (j = 1, N)$ and

$S_{II} \subset (j = 1, N)$; Such that, $S_I \cup S_{II} = S = (j = 1, N)$ and $S_I \cap S_{II} = 0$.

The boundary conditions due to this partial back flow are given by Eqs. (3.9)– (3.12) by taking into account that the inlet and outlet bonnets are adiabatic mixing chambers:

(i) At the inlet cross-section

$$\xi = 0: \quad \sum_{J=1}^{N} \frac{w_{1j}}{\overline{w_1}} \left(\theta_1^- - \theta_{1j}\right) = 0, \quad \theta_1^- = 1, \tag{3.9}$$

And for $w_{1j} > 0 \Rightarrow \theta_{1j} = \theta_{1,forward} = const\left(j \in S_I\right)$.

(ii) At the outlet cross-section

$$\xi = 1: \sum_{j=1}^{N} \frac{w_{1j}}{\overline{w_1}} \left(\theta_{1j} - \theta_1^+\right) = 0, \tag{3.10}$$

and for $w_{1j} < 0 \Rightarrow \theta_{1j} = \theta_{1,back} = const\left(j \in S_{II}\right)$.

For counter flow $\left(NTU_2 > 0; \overline{w_1} > 0\right)$

$$\xi = 1: \quad \theta_2 = 0. \tag{3.11}$$

(iii)For counter flow $\left(NTU_2 > 0;\ \overline{w_1} > 0\right)$

$$\xi = 0: \quad \theta_2 = 0. \tag{3.12}$$

3.4. Axial temperature profiles in a shell and tube heat exchanger considering deviations from tubeside plug flow

Wilfried Roetzel, Chakkrit Na Ranong [2] solved the system of N + 1 differential equations, Eqs. (3.2) and (3.4), numerically or analytically along with boundary conditions, Eqs. (3.6)–(3.12), given by Ranjit Kumar Sahoo , Wilfried Roetzel,[1] to give the cross-sectional and adiabatic mean temperature profiles Using a suitable finite difference method The results obtained are shown in Figs. 3.2 and 3.3.

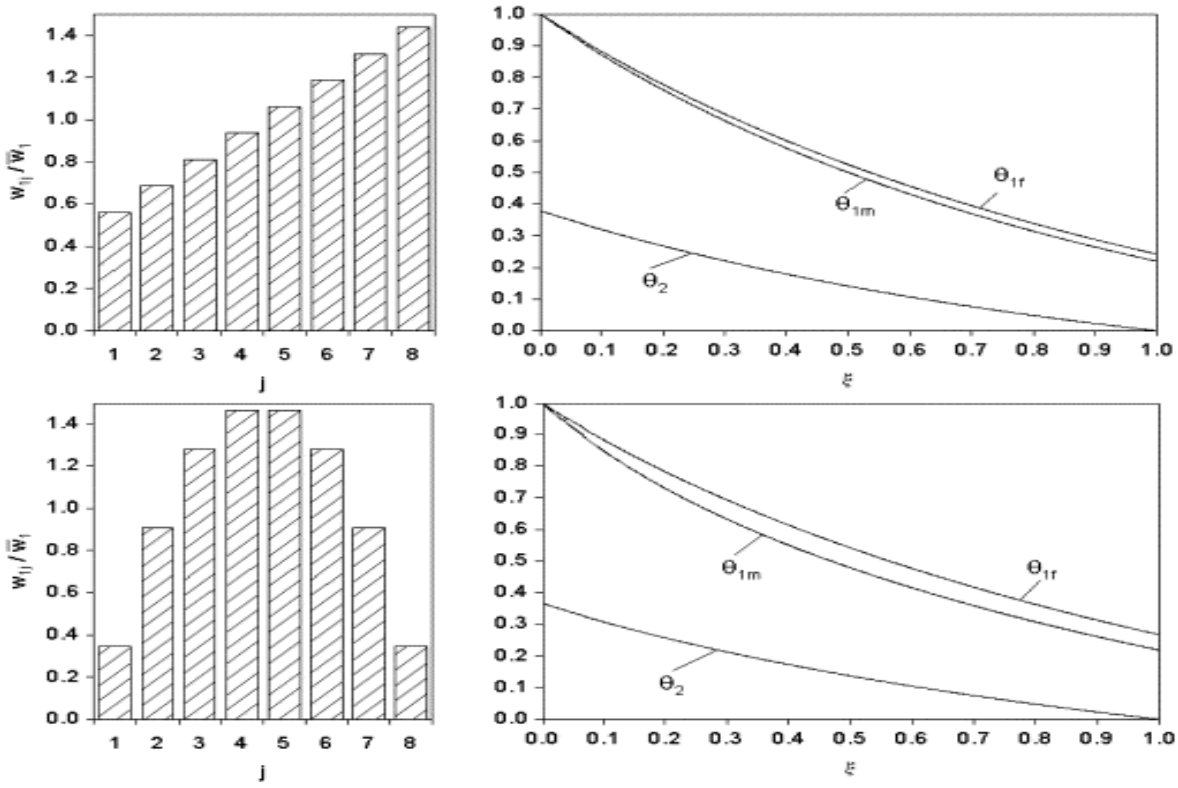

Fig.3.2. Numerically calculated axial temperature profiles for maldistribution without back flow for NTU_1=2 and NTU_2=1. Top: linear velocity distribution; bottom: quadratic velocity distribution

In the heat transfer terminology there appear two mean temperatures: cross-sectional mean and adiabatic mean. The cross-sectional mean temperature is the arithmetic mean value of all tube

side fluid temperatures at a location ξ. The adiabatic mean temperature is the weighted mean of tube side temperatures at a location ξ. The two mean temperatures are expressed as

$$\theta_{1m} = \frac{1}{N}\sum_{j=1}^{N}\theta_{1j}, \tag{3.13}$$

And

$$\theta_{1f} = \frac{1}{N}\sum_{j=1}^{N}\frac{w_{1j}}{\overline{w_1}}\theta_{1j}, \tag{3.14}$$

The cross-sectional mean temperature θ_{1m} is the driving potential for heat transfer whereas the adiabatic mean temperature is the actual exit fluid temperature. These two temperatures are related as

$$\begin{aligned}\theta_{1f} &= \theta_{1m} + \left(\theta_{1f} - \theta_{1m}\right)\\ &= \theta_{1m} + \frac{1}{N}\sum_{J=1}^{N}\left(\frac{w_{1j}}{\overline{w_1}} - 1\right)\theta_{1j}.\end{aligned} \tag{3.15}$$

3.5 Maldistribution without backflow:

First the usual case is considered in which all flow velocities are positive, Fig.3.2. According to Eqs. (3.13) and (3.14) there may arise a difference between the two mean temperatures at the same cross-section of the heat exchanger or not.

There are three thinkable situations:

If the flow velocity is the same for all the channels, i.e. tube side plug flow, there is no difference between the two mean temperatures.

If there is maldistribution but the temperatures are the same for all the channels the two mean temperatures take the same value. This is the case for the cross-section ξ=0, Fig.3.2.

If there is maldistribution and the temperatures are different for some or all of the channels area-averaged temperature and adiabatic mixing temperature are different. For the assumed quadratic velocity distribution the differences are larger than for the assumed linear velocity distribution, Fig. 2. The calculation domain ends at the entrance of the tubeside flowstreams into the outlet bonnet, Fig.3.1. But for a global energy balance of the apparatus the fluid temperature in the

outlet duct 1 is of interest. Because the outlet bonnet is an adiabatic mixing chamber this temperature is θ_{1f}, Fig. 3.2.

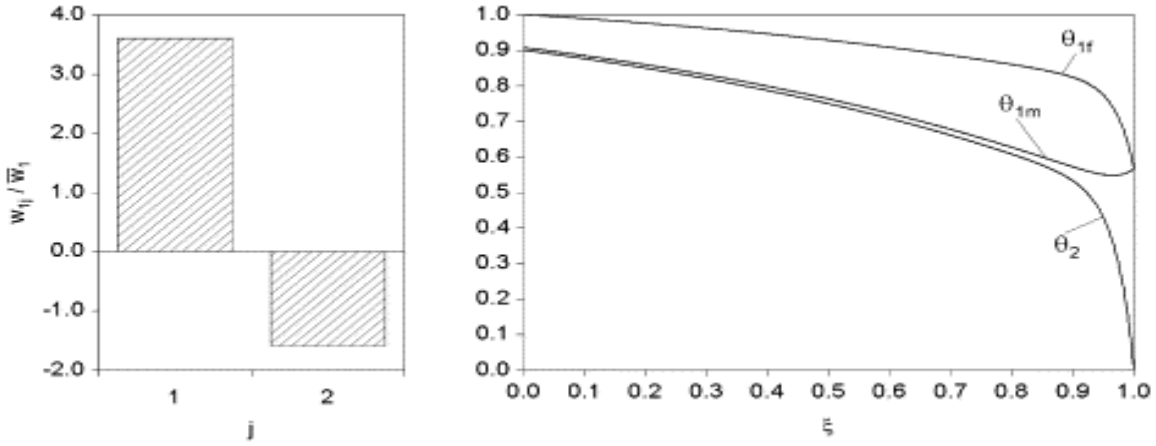

Fig. 3.3.Numerically calculated axial temperature profiles for two channels with back flow in one channel, NTU_1=14.4 and NTU_2=30.

3.6 Backflow:

Cases may arise in which recirculation takes place in the bundle and flow velocities are negative in several tubes. For simplicity two channels are considered with one positive and one negative flow velocity, Fig. 3. In the case of backflow a temperature jump occurs at the beginning of the calculation domain, Fig.3.3, because in the inlet bonnet fluid from the inlet duct 1 with $\theta_{1f}^{-}=1$ is adiabatically mixed with fluid from the backflow channel with $\theta_1(i=1, j=2)<1.$ yielding the fluid inlet temperature of the forward flow channel $\theta_1(i=1, j=1)<1.$ Therefore also the area-averaged temperature at the beginning of the calculation domain falls below 1, Eq. (3.3).

Another characteristic is the minimum followed by a positive slope of the axial profile of the area-averaged temperature. If the forward flow is maldistributed there will be an additional temperature jump at the end of the calculation domain. It is evident from Fig. 3.3 how severe the influence of flow maldistribution on the efficiency of a heat exchanger can be. Under the same operating conditions, i.e. same thermal flow rates, overall heat transfer coeffi- cients and inlet and outlet temperatures, a counterflow heat exchanger with plug flow requires only 11% of the heat transfer area of the 'real' shell and tube heat exchanger with backflow,

Chapter 4

OVERVIEW OF FLUENT

4.1 INTRODUCTION

The availability of affordable high performance computing hardware and the introduction of user-friendly interfaces have lead to the development of commercial CFD packages. Several general-purpose CFD packages have been published in past decade. Prominent among them are: PHONICS [21], FLUENT [12], SRAT-CD [19], CFX [20], FLOW -3D and COMPACT. Most of them are based on the finite volume method.

Among these as mentioned FLUENT is very leading engineering software provides a state of the art computer program for modeling fluid flow and heat transfer in complex geometries. FLUENT provides complete mesh flexibility, solving the flow problems with unstructured meshes that can be generated about complex geometries with relative ease. Supported mesh types include 2D triangular/ quadrilateral, 3D tetrahedral/ hexahedral/ pyramid/ wedge, and mixed (hybrid) meshes.

Fluent also allows refining or coarsening the required mesh based on the flow solution. FLUENT also allows refining or coarsening the required mesh based on the flow solution. FLUENT consists of two main parts. First part is called GAMBIT and second part is called FLUENT the solver.

One can generate the required geometry and grid using GAMBIT. Also one can use T grid to generate a triangular, tetrahedral or hybrid volume mesh from the existing boundary mesh (created by GAMBIT of a third party CAD/CAE package).

Once a grid has been read into FLUENT, all refining operations are performed within the solver. These include the setting boundary conditions, defining fluid properties, executing the solution, refining the grid viewing and post processing the results.

4.2 GAMBIT

Take care to insure that you are in the correct directory. Fire up gambit from the command prompt by typing gambit *filename.* The first thing that you should do is to specify which solver

you need from the Solver menu. Choose 'Fluent 5/6'. This will determine what type of menu popup throughout your session.

Generate a grid

There are two ways of generating a mesh. Gambit calls them 'top down' or 'bottom-up' in the user manuals. These instructions are bottom-up. You will create vertices upon which the edges will be built upon. Connecting edges will create a face. Connecting faces will create a volume (3D). Once the face or volume is created, a mesh can be generated on it. For this example, we will stick to 2D, node -> edge ->face-> mesh. Remember to save and save often.

Vertex:

There are four buttons under the word OPERATIONS in the top right corner of Gambit. They are, from left to right, the *geometry, mesh, zones* and *tools* command. At this time, click on the geometry button. Note: most of the buttons in Gambit toggle off and on. The blank space under the buttons on the right hand side is now showing more buttons and windows. Directly under OPERATIONS is GEOMETRY with 5 buttons: *vertex, edge, face, volume,* and *groups.* Click on the *vertex* button.

By this time, you will have noticed that as you move the mouse over the function buttons a window near the bottom of Gambit tells you what that button does. Use this function to familiarize yourself with the various buttons in Gambit.

Once you have clicked on the *vertex* button more buttons appear below. Click on the button directly below the vertex button called Create Vertex. A floating window called Create Real Vertex appears below. Here you may enter the coordinates of the vertices in your problem. Don't worry about local coordinates at this time. Enter your coordinates in the global area. As you enter in the vertices, they will show up as white X's in the view area. If you cannot see them they may be outside of your viewing area. To remedy this, click on the Fit to Window button, the top left big button in the GRAPHICS/WINDOWS CONTROL area (near bottom right).

If at any time you wish to undo the command you just did, look for the button that has the arrow that is 'spinning' from right to left. The Undo command can undo more than one command, just keep clicking.

For more complicated geometry, such as an airfoil, the vertex data can be imported. Go to File -> Import -> Vertex Data. Enter the path to the file or us the browser. The data file Gambit can read

has to have the file extension .dat. The format of the data in the file must be tab or space delimited.

Most of the data downloaded from the internet will typically need to be modified. There should be no text in addition to the data and a column of zeros for the z -axis will need to be added.

Edges:

Once the vertices are created, you want to create edges connecting them. Under GEOMETRY, click on the edge button (second from left). When the EDGE buttons pop up, right click on the first button on the left. A drop down list will appear giving different options for the edge type. When one of these options is selected a floating window will be displayed. To create smooth curved edges use the NURBS option. There are two methods for the NURBS, interpolate and approximate.

The approximate method with a tolerance of zero will give a smooth curve. To select the vertices for the NURBS line left click the up arrow on the right side of the yellow vertices box. Select the vertices with the mouse and click on the ---> button. Once the vertices are selected, the final one will turn red and the others will turn pink. If the vertices are the ones you want to connect with an edge then click Apply in the floating window. An edge will appear in yellow. Use this procedure to create an edge for the top and bottom of the airfoil and the control volume.

Face:

Under GEOMETRY, click on the *face* button (third from left). When the FACE buttons pop up, click on the first button on the left: Create Face. A floating window called Create Face from Wireframe will appear. Selecting an edge is the same as selecting a vertex. Hold the shift key down and left click on the edge. The edge will turn red. Select a second edge: the first will turn pink and the second will turn red. Select all edges comprising the face and click Apply in the window. A face will be created; its color is light blue. To create a single face from two faces use the Boolean Operations Subtract option.

Mesh:

A mesh can now be created on the face. Under the OPERATION button, click on Mesh Command button. Where the word GEOMETRY used to be, the word MESH will appear with five buttons: *boundary-layer, edge, face, volume* and *group.* You want to mesh the face that you have just created, so click on *face.* Click on the top left button in the FACE menu area, the button is called: Mesh Faces. This will cause the Mesh Faces floating window to pop up. Let everything stay at its default, select the face and click Apply. Gambit may hesitate while it's thinking and then you will see the mesh in yellow. You can play around with mesh spacing but keep the elements and type at Gambits default setting.

Boundary Conditions:

You can set or change the boundary conditions in Fluent but you can also do it in Gambit, in fact, it's a little bit easier. Up in the OPERATIONS menu; click on the Zones button. Under the word ZONES two buttons will appear: Specify Boundary Types and Specify Continuum. Click on the Specify Boundary Types button. A floating window called Specify Boundary Types will appear. Make sure that at the top of this window the solver name 'Fluent 5/6' appears, if not go to the solver menu and choose 'Fluent 5/6'. You must have this correct as different solvers specify BC's differently.

Change the Entity pop down menu to edges. Select the edge that will be the velocity inlet and under the Type pop down menu choose Velocity Inlet. It is recommended that you label the different edges. This will help you keep track of them in the Fluent output reports. The labels must be one word, i.e. no spaces or tabs. To finish creating the BC click *Apply.* Now select the edge that will be the outlet and choose Outflow. The top and bottom edges of the airfoil and control volume are Walls. There is a list at the top of this window that should reflect the two BC's that you have created.

Save and Export:

The file that you have been saving to throughout the session is a Gambit file and is different from a mesh file. To create the mesh file for Fluent to import click on File-> Export-> Mesh. The next pop up window will have file type (UNS/RAMPANT /FLUENT 5) and file

name. Type in the name as you please but keep the .msh file name extension. If the geometry is 2D, then check the box “Export 2d Mesh”.

4.3 NUMERICAL SOLVING TECHNIQUE

FLUENT in general solve the governing integral equations for the conservation of mass and momentum, and (when appropriate) for energy and other scalars such as turbulence and chemical species. Usually control volume based technique is used that consists of:

- Division of the domain into discrete control volumes using a computational grid.
- Integration of the governing equations on the individual control volumes to construct algebraic equations for the discrete dependent variables (“unknowns”) such as velocities, pressure, temperature and conserved scalars.

Linearization of the discretized equations and solution of the resultant linear equation system to yield updated values of the dependent variables.

Solution Methodology

FLUENT allows choosing either of two numerical methods:

- Segregated solver
- Coupled solver

The two numerical methods employ a similar discretization process (finite volume), but the approach used to linearize and solve the discretized equation is different**.**

Segregated Method

Using this approach, the governing equations are solved sequentially (i.e., segregated from one another). Because the governing equations are non-linear (and coupled), several iterations of the solution loop must be performed before a converged solution is obtained. Each iteration consists of the steps illustrated below:

1. Fluid properties are updated, based on the current solution. (if the calculation has just begun, the fluid properties will be updated based on the initialized solution).
2. The $u, v \, and \, w$ momentum equations are each solved in turn using current values for pressure and face mass fluxes, in order to update the velocity field.
3. Since the velocities obtained in step 2 may not satisfy the continuity equation locally, a "Poisson-type" equation for the pressure correction is derived from the continuity equation is then solved to obtain the necessary corrections to the pressure and velocity fields and the face mass fluxes such that continuity is
4. Where appropriate, equations for scalars such as turbulence, energy, species and radiation are solved using the previously updated values of the other variables.
5. When inter-phase coupling is to be included, the source terms in the appropriate continuous phase equations may be updated with a discrete phase trajectory calculation.

These steps are continued until the convergence criteria are met.

Coupled Method

The coupled solver solves the governing equations of continuity, momentum and (where appropriate) energy and species transport simultaneously (i.e., coupled together). Governing equations for additional scalar will be solved sequentially (i.e., segregated from one another and from the coupled set) using the procedure described for the segregated solver. Because the governing equations are non-linear (and coupled), several iterations of the solution loop must be performed before a converged solution is obtained. Each iteration consists of the steps outlined below:

1. Fluid properties are updated, based on the current solution. (If the calculation has just begun, the fluid properties will be updated based on the initialized solution).
2. The continuity, momentum and (where appropriate) energy and species equations are solved simultaneously.
3. Where appropriate, equations for scalars such as turbulence and radiation are solved using the previously updated values of the other variables.
4. When interphase coupling is to be included, the source terms in the appropriate continuous phase equations may be updated with a discrete phase trajectory calculation.
5. A check for convergence of the equation set is made.

These steps are continued until the convergence criteria are met.

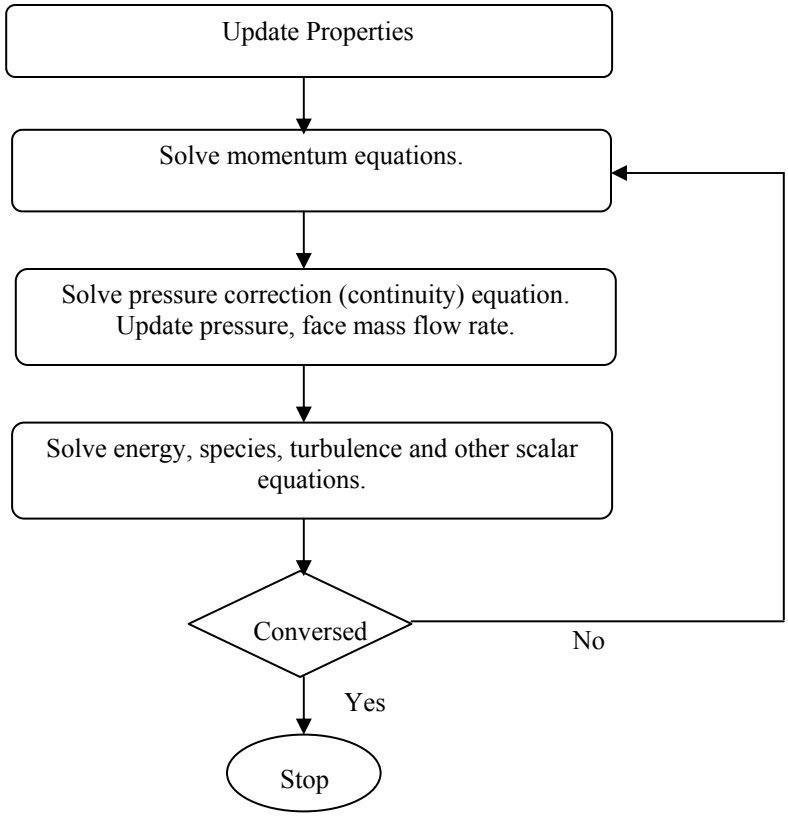

Figure4.1: Overview of the Segregated Solution Method

Linearization: Implicit & Explicit

In both the segregated and coupled solution methods the discrete, non-linear governing equations are linearized to produce a system of equations for the dependent variables in every computational cell. The resultant linear system is then solved to yield an updated flow-field solution.

The manner in which the governing equations are linearized may take an "implicit" or "explicit" form with respect to the dependent variables (or set of variables) of interest. By implicit or explicit we mean the following:

- **Implicit:** for a given variable, the unknown value in each cell is computed using a relation that includes both existing and unknown values from neighbouring cells.

Therefore each unknown will appear in more than one equation in the system, and these equations must be solved simultaneously to give the unknown quantities.

- **Explicit:** for a given variable, the unknown value in each cell is computed using a relation that includes only existing values. Therefore each unknown will appear in only one equation in the system, and the equations for the unknown value in each cell can be solved one at a time to give the unknown quantities.

In the segregated solution method each discrete governing equation is linearized only by implicitly with respect to that equations dependent variable. This will result in a system of linear equations with one equation for each cell in the domain. For example, the x-momentum equation is linearized to produce a system of equations in which u velocity is the unknown. Simultaneous solution of this equation system (using the scalar AMG solver) yields an updated u velocity field.

In the coupled solution method user have a choice of using either an implicit or explicit Linearization of the governing equations. Governing equations for additional scalars that are solved segregated from the coupled set, such as for turbulence, radiation etc., linearized and solved implicitly using the same procedures as in the segregated solution method.

If one choose the implicit option of the coupled solver, each equation in the coupled set of governing equations is linearized implicitly with respect to all dependent variables in the set. This will result in a system of linear equations with N equations for each cell in the domain, where N is the number of coupled equations in the set. For example, Linearization of the coupled continuity, *x, y, z* momentum and energy equation set will produce a system of equations in which $\rho, u, v, w \text{ and } T$ are the unknowns. Simultaneous solution of this equation system (using the block AMG solver) yields at once updated pressure, *u, v, w* velocity and temperature fields.

If one chooses the explicit option of the coupled solver, each equation in the coupled set of governing equations is linearized explicitly. As in the implicit option, this will result in a system of equations with N equations for each cell in the domain. And likewise, all dependent variables in the set will be updated at once. However, this system of equations is explicit in the unknown dependent variables. For example, the x-momentum equation is written such that the updated x velocity is a function of existing values of the field variables. Because of this, a linear equation solver is not needed. Instead, the solution is updated using a multi stage (Runge-kutta) solver.

In summary, the coupled explicit approach solves for all variables (ρ, u, v, w, T) one cell at a time.

Discretization

Fluent uses a control volume based technique to convert the governing equations to algebraic equations that can be solved numerically. This control volume technique consists of integrating the governing equations about each control volume, yielding discrete equations that conserve each quantity on a control volume basis.

Initializing the Solution

As because solving is done by iterative method, user must provide FLUENT with an initial "guess" for the solution flow field. In many cases, one must take extra care to provide an initial solution that will allow the desired final solution to be attained.

There are two methods for initializing the solution:

- Initialize the entire flow field (in all cells).
- Patch values or functions for selected flow variables in selected cell zones or "registers" of cells.

Convergence and Stability

Under Relaxation

Because of the nonlinearity of the equation set being solved by FLUENT, it is necessary to control the change of ϕ. This is typically achieved by under relaxation, which reduces the change of ϕ produced during each iteration.

By controlling relaxation factor one can avoid the sudden divergence in the solving process.

Monitoring Residuals

During the solution process one can monitor the convergence dynamically by checking residuals, statistics, force values, surface integrals, and volume integrals.

Judging the convergence

At the end of each iteration, the residual sum for each of the conserved variables is computed. On a computer with infinite precision, these residuals will go to zero as the solution converges. On an actual computer, the residuals decay to some small value ("round off") and

then stop changing ("level out"). For "single precision" computations (the default for workstations and most computers), residuals can drop as many as six orders of magnitude before hitting round off. Double precision residuals can drop up to twelve orders of magnitude. Residual definitions that are useful for one class of problem are sometimes misleading for other classes of problems. Therefore it is a good idea to judge convergence not only by examining residual levels, but also by monitoring relevant integrated quantities such as drag or heat transfer coefficient.

4.4 PROBLEM SOLVING STEPS

After determining the important features of the problem following procedural steps are followed for solving it

1. Create the geometry model and mesh it.
2. Start the appropriate solver for 2D or 3D modeling.
3. Import the grid and check it.
4. Select the solver formulation
5. Chose the basic equation to solved: laminar or turbulent (or in viscid), chemical species or reaction, heat transfer models, etc. Also identify additional models needed: fans, heat exchangers, porous media, etc.
6. Specify the material properties.
7. Specify the boundary properties.
8. Adjust the solution control parameter.
9. Initialize the flow field.
10. Calculate a solution.
11. Examine the results.
12. Save the results.
13. If necessary, refine the grid or consider revisions to the numerical or physical model.

Chapter 5

GOVERNING EQUATIONS AND NUMERICAL SIMULATION

5.1 Introduction

Due to the advances in computational hardware and available numerical methods, CFD is a powerful tool for the prediction of the fluid motion in various situations, thus, enabling a proper design. CFD is a sophisticated way to analyze not only for fluid flow behavior but also the processes of heat and mass transfer.

Advances in physical models, numerical analysis and computational power enable simulation of the heat transfer characteristics in three-dimensional circumstances. A three dimensional approximation of a turbulent flow is chosen to explore since the three-dimensional approach is considerably greater than two dimensional and moreover, a turbulent flow is fundamentally three-dimensional.

Owing to extremely long computation times, detailed studies on the tubular heat exchanger in three-dimensional flow are very uncommon. Hence, the simulation of the three-dimensional flow field under complex geometrical conditions is seemingly intricate and challenging task.

The available computational fluid dynamics software package FLUENT is used to determine the related problems. FLUENT uses a finite volume method and requires from the user to supply the grid system, physical properties and the boundary conditions. When planning to simulate a problem, basic computation model considerations such as boundary conditions, the size of computational domain, grid topology, two dimensions or three-dimension model, are necessary. For example, appropriate choice of the grid type can save the set up time and computational expense. Moreover, a careful consideration for the selection of physical models and determination of the solution procedure will produce more efficient results. Dependent on the problem, the geometry can be created and meshed with a careful consideration on the size of the computational domain, and shape, density and smoothness of cells. Once a grid has been fed into

FLUENT, check the grids and executes the solution after setting models, boundary conditions, and material properties. FLUENT provides the function for post processing the results and if necessary refined the grids is available and solve again as the above procedure. As described in the objective, the purpose of this study is to investigate numerically the effect of maldistribution in the tubular heat exchanger.

5.2. Governing Equations

The flow and temperature field in the model geometry is determined by the continuity equation, the complete unsteady Navier-Stokes and the energy equation for incompressible fluid with temperature-dependent properties. These three-dimensional equations, to be solved by numerical calculations in the Cartesian coordinates, are as follows:

Continuity equation:
$$\frac{\partial \rho}{\partial t} + \frac{\partial}{\partial x_i}(\rho u_i) = 0 \tag{5.1}$$

Momentum equation:
$$\frac{\partial}{\partial t}\left(\rho u_i u_j\right) = -\frac{\partial \rho}{\partial x_i} + \frac{\partial \tau_{ij}}{\partial x_j} \tag{5.2}$$

Where
$$\tau_{ij} = \mu\left(\frac{\partial u_i}{\partial x_j} + \frac{\partial u_j}{\partial x_i}\right) - \frac{2}{3}\frac{\mu \partial u_k}{\partial x_k}\delta_{ij} \tag{5.3}$$

Energy equation :
$$\frac{\partial}{\partial t}(\rho E) + \frac{\partial}{\partial x_i}\left(u_i\left(\rho E + \rho\right)\right) = \frac{\partial}{\partial x_i}\left(k\frac{\partial T}{\partial x_i}\right) \tag{5.4}$$

Where E is the total energy and k is the thermal conductivity.

Navier-Stokes Equations in a Turbulent Flow Regime:

The Navier-Stokes equations mentioned thus far have been developed essentially for laminar flow regimes. However, in practical applications, flow is almost always turbulent. To compensate for this fact a model needs to be utilized to simulate turbulence. Turbulence is fundamentally the presence of velocity fluctuations within flow. It is characterized by random,

three-dimensional motions of fluid particles in addition to the mean motion (Fox & McDonald 1992). Due to the actuality of the velocity fluctuations being random and high frequency leads to the consequence that the study of turbulence is very difficult. Different methods, which are employed to estimate turbulence, are described in the following sections.

The Standard k–ε Model:

The transport equations for the standard k–ε model are given in Equation 5.12 and 5.13. The derivation of these is complex and shall be left to reference books such as Wilcox (1993). An unpretentious statement of the origins of the partial differential equations is that the principle of energy balance is manipulated which is not accounted for in simple algebraic approximations. The main assumption in this model is that turbulence is simulated by an increase in the viscosity of the fluid.

$$\frac{\partial \rho k}{\partial t}+\frac{\partial \rho \overline{u_j} k}{\partial x_j}=\frac{\partial}{\partial x_j}\left[\mu \frac{\partial k}{\partial x_j}\right]-\frac{\partial}{\partial x_j}\left(\frac{\rho}{2}\overline{u_j' u_i' u_i'}+\overline{p' u_j'}\right)- \overline{\rho u_i' u_j'}\frac{\partial \overline{u_i}}{\partial x_j}-\mu \overline{\frac{\partial u_i'}{\partial x_k}}\overline{\frac{\partial u_i'}{\partial x_k}} \tag{5.12}$$

$$\frac{\partial(\rho\varepsilon)}{\partial t}+\frac{\partial(\rho u_j \varepsilon)}{\partial x_j}=C_{\varepsilon 1}P_k\frac{\varepsilon}{k}-\rho C_{\varepsilon 2}\frac{\varepsilon^2}{k}+\frac{\partial}{\partial x_j}\left(\frac{\mu_t}{\sigma_\varepsilon}\frac{\partial \varepsilon}{\partial x_j}\right) \tag{5.13}$$

The individual terms in these equations as given by Hutchins-Sach (1999) are

$\frac{\partial \rho k}{\partial t}$ = Fluctuation of k

$\frac{\partial \rho \overline{u_j} k}{\partial x_j}$ = Convection of k

$\frac{\partial}{\partial x_j}\left[\mu \frac{\partial k}{\partial x_j}\right]$ = Molecular diffusion of k

$-\frac{\partial}{\partial x_j}\left(\frac{\rho}{2}\overline{u_j' u_i' u_i'}+\overline{p' u_j'}\right)$ = Turbulent diffusion of k

$-\overline{\rho u_i' u_j'}\frac{\partial \overline{u_i}}{\partial x_j}$ = Rate of production of k

$-\mu\frac{\overline{\partial u_i'}}{\partial x_k}\frac{\overline{\partial u_i'}}{\partial x_k}$ = Dissipation of k

$\frac{\partial(\rho\varepsilon)}{\partial t}$ = Unsteady function of ε

$\frac{\partial(\rho u_j \varepsilon)}{\partial x_j}$ = Convection of ε

$C_{\varepsilon 1}P_k\frac{\varepsilon}{k}$ = Dissipation increase due to production of k

$-\rho C_{\varepsilon 2}\frac{\varepsilon^2}{k}$ = Dissipation of ε

$\frac{\partial}{\partial x_j}\left(\frac{\mu_t}{\sigma_\varepsilon}\frac{\partial \varepsilon}{\partial x_j}\right)$ = viscous destruction of ε

The turbulent viscosity is given as

$$\mu_t = \rho C_\mu \sqrt{kL} = \rho C_\mu \frac{k^2}{\varepsilon} \tag{5.14}$$

The parameters introduced and their common values are

$C_\mu = 0.09$; $C_{\varepsilon 1} = 1.44$ $C_{\varepsilon 2} = 1.92$ $\sigma_k = 1.0$ $\sigma_\varepsilon = 0.09$

This model's popularity arises from its robustness, satisfactory accuracy and low computational effort. Its weakness lies in that it is a semi-empirical model and the derivation of the model equations relies on phenomenological considerations and empiricism (Fluent 1998).

5.3 Numerical Simulation:

A difficulty for application of the numerical methods in tubular heat exchangers is the fact that one is faced with a complex geometry of the flow configuration. Furthermore, several geometric parameters directly effecting on the enhancement of heat transfer.

5.3.1. Grid Generation

In this study, the geometries of the problems are carefully constructed. All cases were modelled and meshed with the GAMBIT. FLUENT also comes with the CFD program that allows the user to exercise the complete flexibility to accommodate the compatible complex geometries. The refinement and generation of the grid system is important to predict the heat transfer in complex geometries. In other words, density and distribution of the grid lines play a pivotal role to generate accuracy. Due to the strong interaction of mean flow and turbulence, the numerical results for turbulent flows tend to be more dependent on grid optimization than those for laminar flow

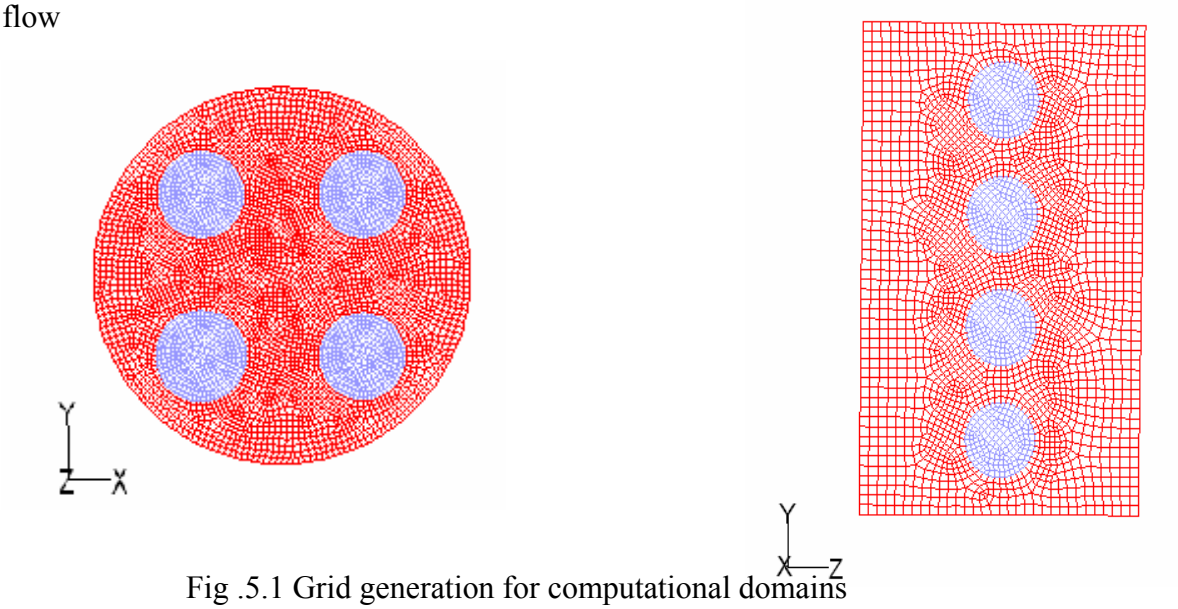

Fig .5.1 Grid generation for computational domains

5.3.2. Choosing the Physical Properties:

The definition of physical properties (density, specific heat, thermal conductivity, viscosity) of fluids and solids is a necessary factor for setting up the model. In this study, hot water is flowing through the tubes and cold water is flowing through the shell. The physical properties of hot water and cold water are listed in the table

Table: 5.1. Physical Properties of water

	Hot water at 357 K.	Cold water at 283 K
Density (Kg/m^3)	971.4	1001
Specific heat (j/Kg K)	4199.2	4197
Thermal conductivity (w/m .k)	0.67104	0.5751
viscosity	0.000339	0.001368

5.3.3. Boundary Conditions:

In order to evaluate the heat and momentum transfer of tubular heat exchanger tube bundles, some preliminary conditions of the physical model have to be defined appropriately. For the numerical approach to the problem, the boundary conditions are required to set for all boundaries of the computational domain.

	Hot fluid side	Cold fluid side
In let condition	Mass flow inlet	Mass flow inlet
Out let condition	Out flow	Out flow

5.3.4. Control Parameters:

It is noteworthy that proper numerical control and modelling techniques are necessary for to speed up convergence and stability of the calculation. With a controlvolume- based technique, FLUENT converts the governing equations to algebraic forms that can be solved numerically. This control volume technique consists of integrating the governing equations inside each control volume, yielding discrete equations that conserve each quantity on a control-volume basis. For discretization of equations, the user needs to select the respective numerical schemes. The first order upwind numerical scheme is selected to simulate the problems.

For the aspect of pressure-velocity coupling, The Pressure-Implicit with Splitting of Operators (SIMPLE) is selected. SIMPLE pressure-velocity coupling scheme is a part of the SIMPLE family and it is highly recommended for all steady flow calculations. SIMPLE is based on the higher degree of the approximate relation between the corrections for pressure and velocity. An approach to judging convergence is setting as the convergence criterion.

5.3.5. Algorithm:

In order to simulate, the following procedures of analysis are performed:

1. Start the FLUENT with 3D solver
2. Read an existing grid file and feed into FLUENT
3. Check the grid (e.g., concerning the dimension of the calculation domain, the cell volume, the number of nodes and area of each cell)
4. Choose the suitable type of solver:

Fluent supplies three types of solver for solving the discrete equation. Basically, the specific characteristics of the investigation (incompressible and mildly compressible flows) are dealt with "segregated solver". This solver solves the continuity, momentum, energy and species equations sequentially (i.e., Segregated from one another) while the other two solvers solve these equations simultaneously (i.e., coupled together) applied for high-speed compressible flow. Here the segregated solver has been selected.

5. Choose the model: To calculate the flow field, select the k- ε (standard) model. For coupling heat transfer (convection and conduction), activate the energy equation.

6. Define the properties of following material:

- Physical properties of water

7. Define the boundary conditions (see section 4.3.5)

8. Define the control parameter:

The following under-relaxation factors are set.

- Pressure 0.3
- Energy 1.0
- Momentum 0.7
- Turbulent kinetic energy 0.8
- Turbulent dissipation rate 0.8

Select the reference of discretization of differential equations,

- For pressure choose, STANDARD
- For momentum choose, First order upwind
- For pressure-velocity coupling choose, SIMPLE
- For energy choose, First order upwind
- For turbulent kinetic energy choose, First order upwind
- For turbulent dissipation rate choose, First order upwind

Set the convergence criteria,

Continuity = 0.001 k = 0.001 ε = 0.001

x, y, z velocity = 0.001 Energy = 1e-6

9. Initialization of flow field.

10. Calculate the solution.

11. Save the result.

Chapter 6

RESULTS AND DISSCUSSIONS

6.1 Introduction

This chapter mostly deals with the results of the investigations of the area weighted and mass weighted temperature profiles for with out back flow and with back flow in tubular heat exchangers.

Evaluation of mass weighted and area weighted average temperatures

FLUENT evaluates the mass weighted and area weighted temperatures as follows:

Mass weighted average temperature

The mass-weighted average of a temperature is computed by dividing the summation of the product of the selected temperature and the absolute value of the dot product of the facet area and momentum vectors by the summation of the absolute value of the dot product of the facet area and momentum vectors (surface mass flux):

The fluid mass weighted temperature was calculated at any position of the calculation domain.

$$T_{ad} = \frac{\int T \rho \overline{u} . d \overline{A}}{\int \rho \overline{u} . d \overline{A}} = \frac{\sum_{i=1}^{n} T_i \rho_i \overline{u}_i . \overline{A}_i}{\sum_{i=1}^{n} \rho_i \overline{u}_i \overline{A}_i}$$

The area-weighted average of a temperature is computed by dividing the summation of the product of the selected temperature and facet area by the total area of the surface:

$$T_m = \frac{1}{A} \int T \, d A = \frac{1}{A} \sum_{i=1}^{n} T_i \left| A_i \right|$$

6.2 single-pass shell-and-tube exchanger with four channels:

6.2.1Case1: with pure axial plug flow on the shell side and maldistribution without back flow on the tube side:

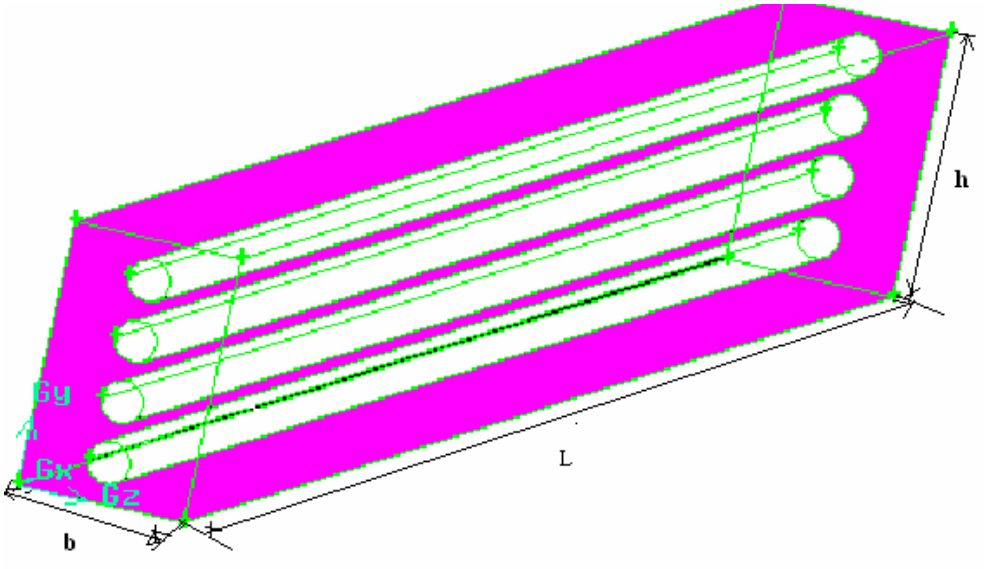

Fig: 6.1: Computational domain for four tube in-line arrangement

Dimensions of the exchanger:

Length of the exchanger (L)	560 mm
Width of the exchanger (b)	52 mm
Height of the exchanger (h)	32 mm
Tube diameter (d)	8 mm

Boundary conditions:

Channel number	Mass flow rate in (kg/sec)
Channel 1	5.124
Channel 2	3.416
Channel 3	1.708
Channel 4	0

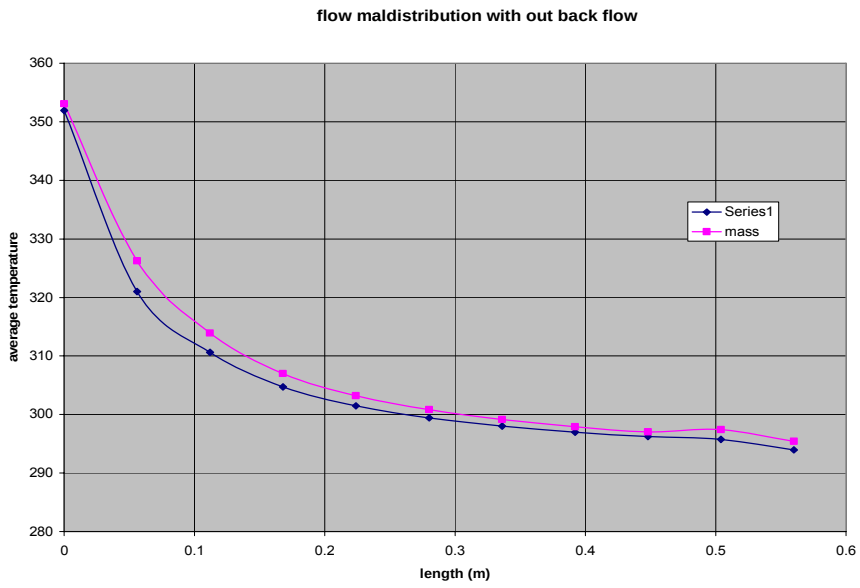

Fig. 6.2: Average temperature profiles for maldistribution without back flow for four tube in-line arrangement

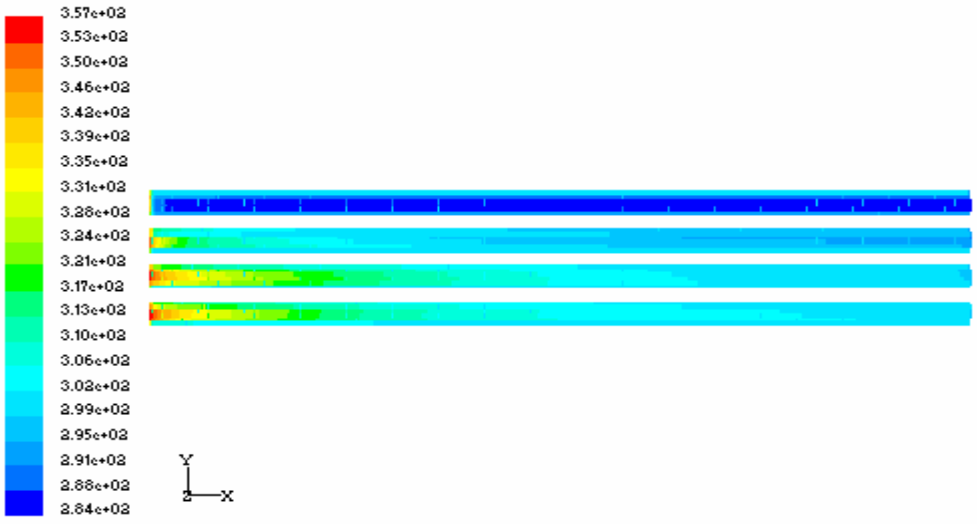

Fig. 6.3: Temperature contours for maldisribution with out back flow for four tube in-line arrangement

6.2.2 Case2:

The flow velocity is the same for all the channels, i.e. tube side plug flow, The constant mass flow rate, 2.562, Kg/sec is given in each of the four channels. In this case both area weighted average and mass weighted average temperatures are identical which are listed in the table (6.2).

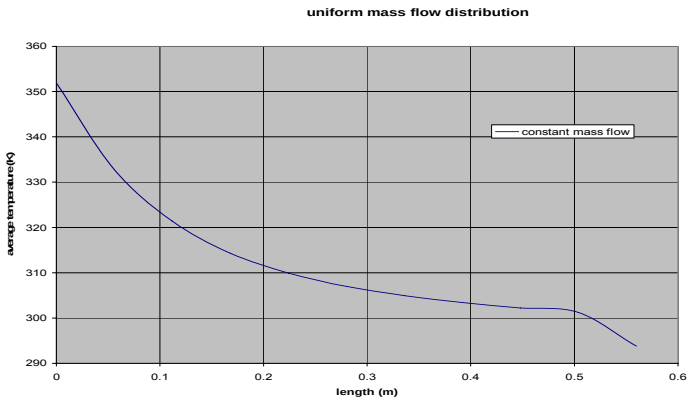

Fig: 6.4: Average temperature profile for uniform mass flow distribution for four tube in-line arrangement

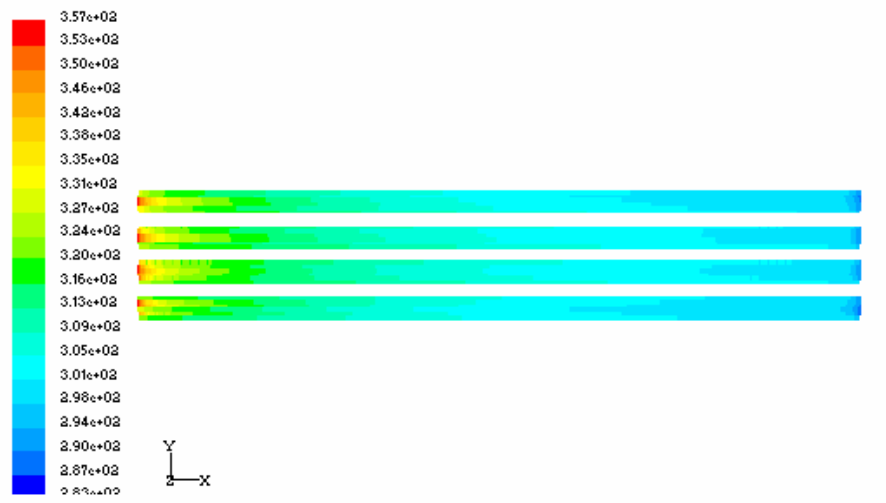

Fig.6.5: Temperature contours for uniform mass flow distribution for four tube in-line arrangement

Table 6.1: Average temperatures for maldistribution with out back flow and uniform mass flow distribution

Length	Area weighted average temperature for with out back flow (K)	Mass weighted average temperature for with out back flow(K)	temperature for uniform form mass flow distribution (K)
0	351.92123	351.92123	351.92123
0.056	321.00366	326.22189	332.7937
0.112	310.6395	313.9133	321.3988
0.168	304.71317	306.99814	314.33673
0.224	301.46387	303.21677	309.91846
0.28	299.4227	300.8208	307.00452
0.336	297.99478	299.13965	304.95154
0.392	296.95926	297.92462	303.41559
0.448	296.20728	297.0444	302.20953
0.504	295.72238	296.4097	301.2261
0.56	293.97058	294.42264	293.80063

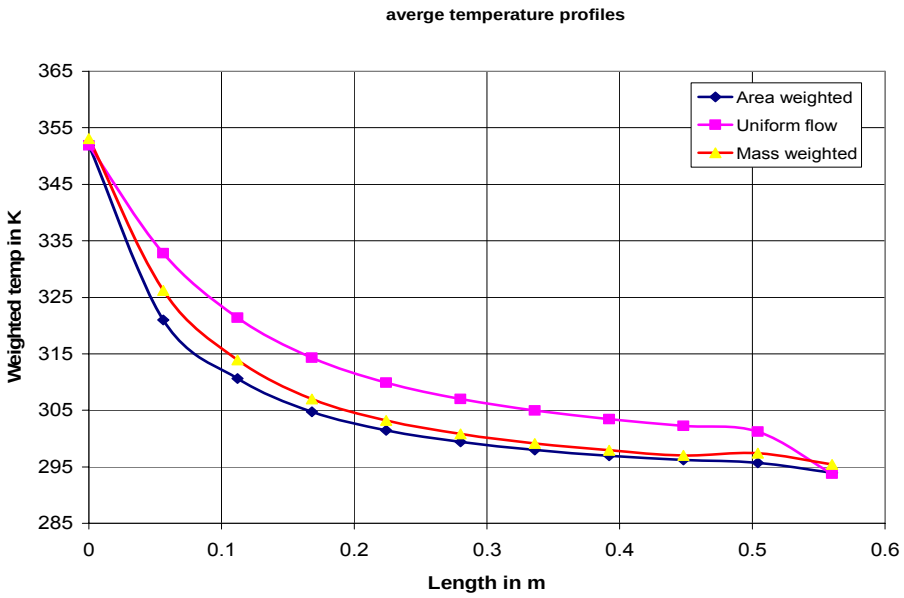

Fig: 6.6: Average temperature profiles for both maldistribution and uniform mass flow distribution for four tube in-line arrangement

6.2.3. Case 3: With pure axial plug flow on shell side and maldistribution with back flow on tube side:

Back flow may arise in which recirculation takes place in the bundle and flow velocities are negative in several tubes. For simplicity two channels are considered with one positive and one negative flow velocity. Dimensions of computational domain:

Length of the exchanger (L)	560 mm
width of the exchanger (b)	24 mm
Height if the exchanger (h)	28 mm
Tube diameter (d)	8 mm

Boundary conditions:

Channel number	Mass flow rate in (kg/sec)
Channel 1	5.856
Channel 2	2.928

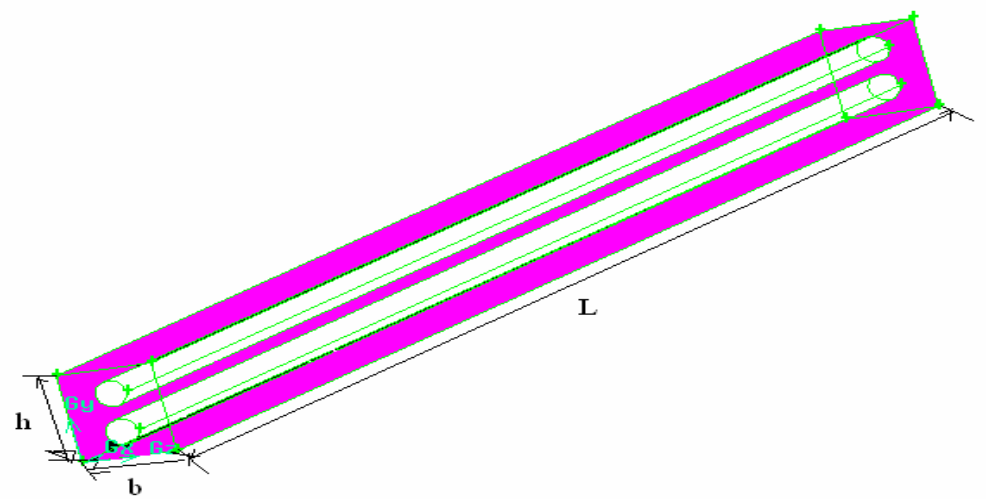

Fig: 6.7: Computational domain for two tube in-line arrangement

In the case of backflow a temperature jump occurs at the beginning of the calculation domain, because in the inlet bonnet fluid from the inlet duct 1 with $\theta_{1f}^{-}=1$ is adiabatically mixed with fluid from the backflow channel with $\theta_1(i=1, j=2)<1$. yielding the fluid inlet temperature of the forward flow channel $\theta_1(i=1, j=1)<1$. Therefore also the area-averaged temperature at the beginning of the calculation domain falls below 1, Another characteristic is the minimum followed by a positive slope of the axial profile of the area-averaged temperature. If the forward flow is maldistributed there will be an additional temperature jump at the end of the calculation domain.

Table 6.2: Average temperatures for maldistribution with back flow and uniform mass flow distribution

Length	Area weighted average temperature for back flow (K)	Mass weighted average temperature for back flow(K)	temperature for uniform flow(K)
0	318.22501	336.62564	352.75647
0.056	319.73785	328.50537	336.46866
0.112	316.05399	315.90933	327.54349
0.168	313.80304	313.55865	321.68304
0.224	313.11194	313.09424	317.48221
0.28	312.78152	312.80569	314.31009
0.336	312.73172	312.7482	311.78931
0.392	312.72986	312.73856	309.68646
0.448	312.72812	312.73273	307.86093
0.504	312.72495	312.72739	306.22003
0.56	306.32108	296.90686	295.21585

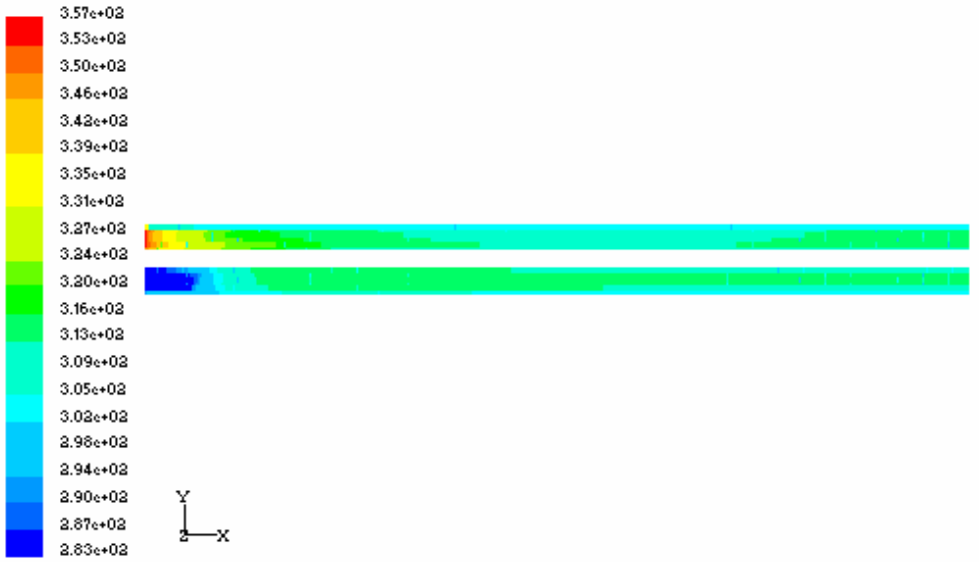

Fig 6.8: Temperature contours for maldistribution with back flow for two tube in-line arrangement

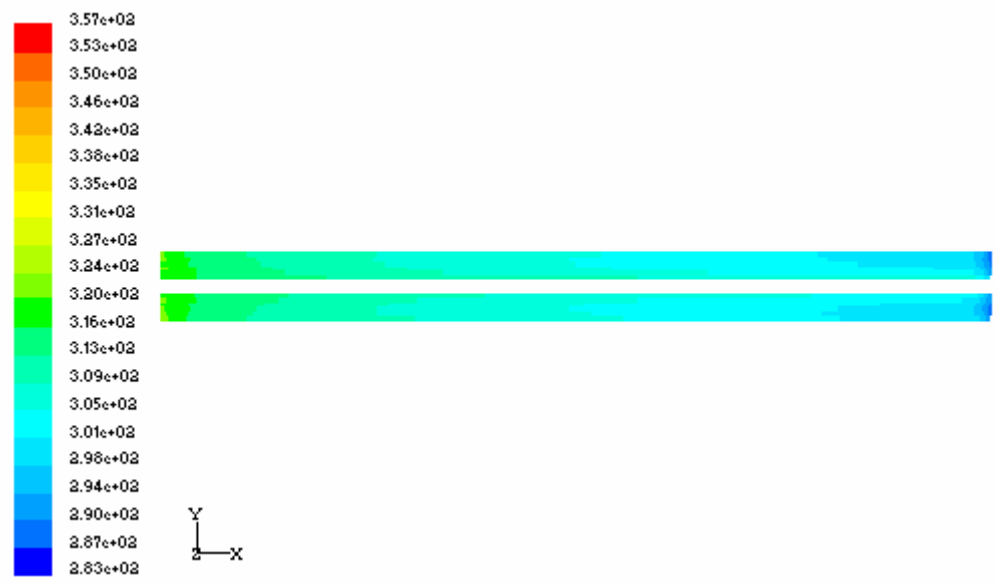

Fig 6.9: Temperature contours for uniform mass flow distribution for two tube in-line arrangement

6.3. single-pass shell-and-tube heat exchanger with square in-line tube Arrangement

Case1: with pure axial plug flow on the shell side and maldistribution with out back flow on the tube side:

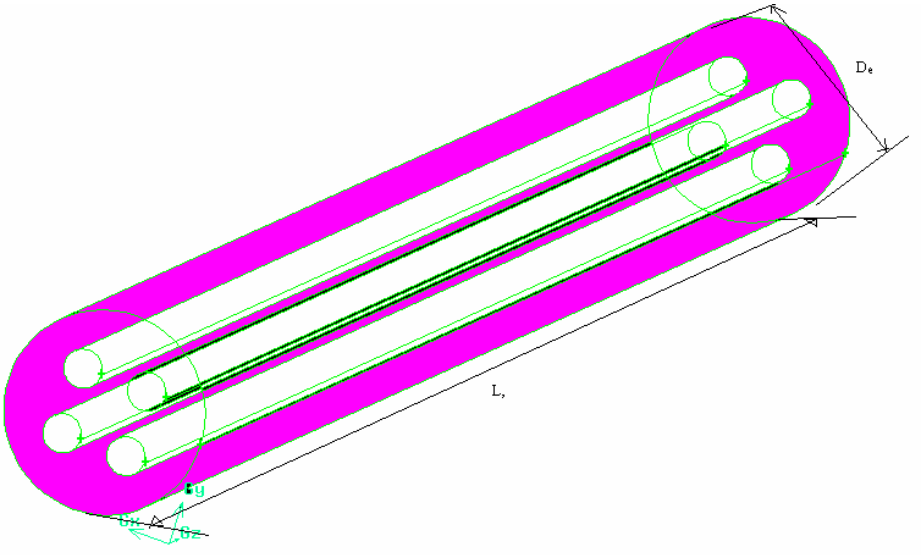

Fig: 6.10. Computational domain for square inline-tube arrangement

Dimensions of the computation domain:

Length of the exchanger (L)	560 mm
Shell diameter (D)	42 mm
Tube diameter (d)	8 mm

Boundary conditions:

Channel number	Mass flow rate in (kg/sec)
Channel 1	5.124
Channel 2	3.416
Channel 3	1.708
Channel 4	0

Table 6.3: Average temperatures for maldistribution without back flow

Length (m)	Area weighted average temperature for with out back flow (K)	Mass weighted average temperature for with out back flow(K)	temperature for uniform form mass flow distribution (K)
0	353.28769	353.28769	353.28769
0.056	319.23352	326.7395	331.11636
0.112	309.27524	313.5257	320.41678
0.168	303.53833	305.96405	313.55688
0.224	301.1683	302.77414	308.77625
0.28	300.47263	301.4223	305.85608
0.336	299.90469	300.4129	304.18185
0.392	299.36362	299.41894	302.85172
0.448	298.84195	298.81024	301.34631
0.504	298.41284	298.38641	300.26743
0.56	295.41818	295.50723	294.82794

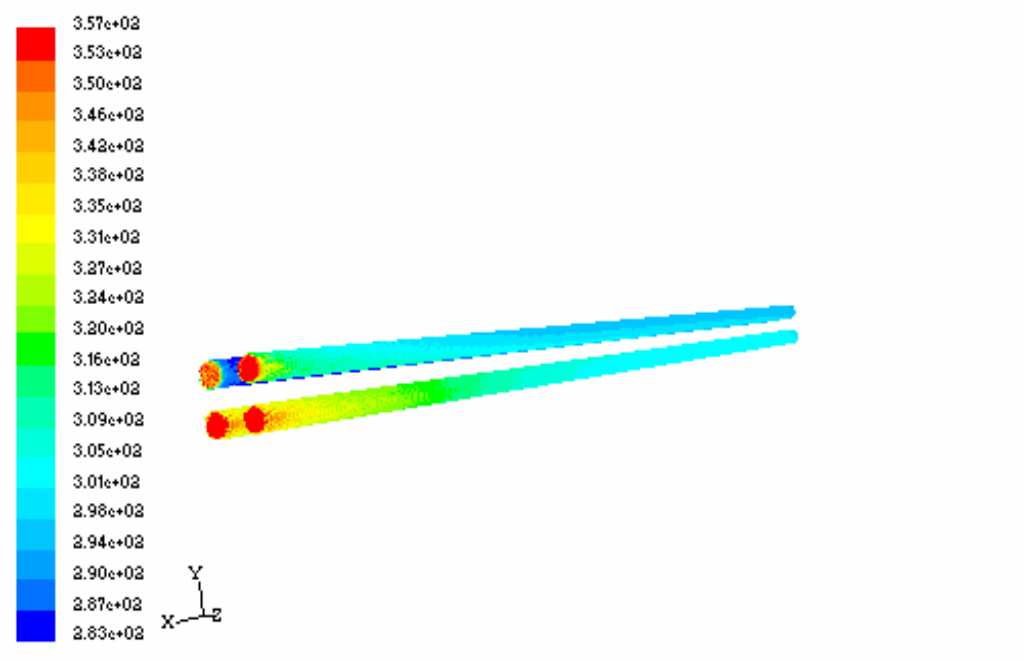

Fig: 6.11. Temperature contours for maldistribution with out back flow for square in-line tube arrangement

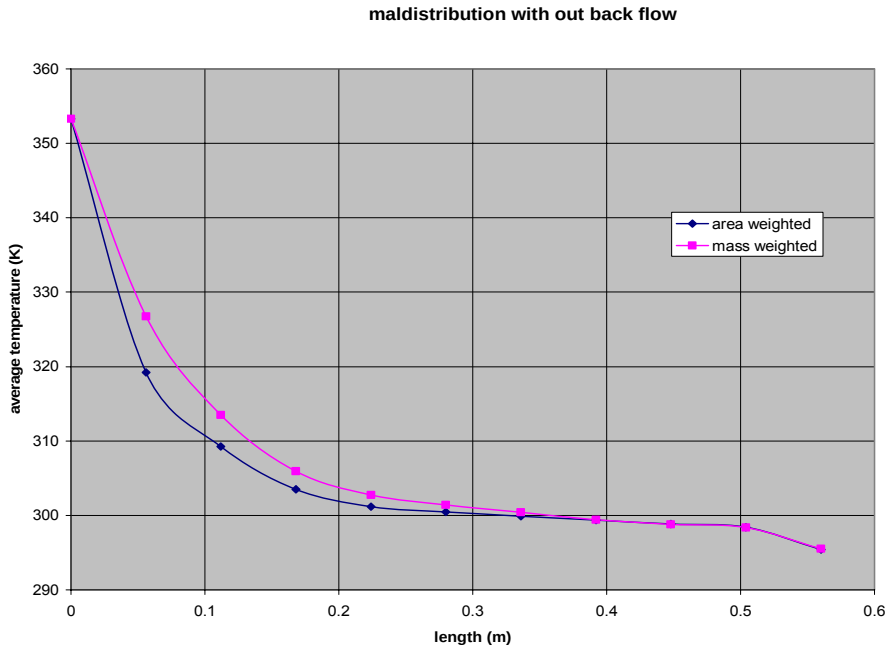

Fig: 6.12: Temperature profiles for maldistribution with out back flow for Square in-line tube arrangement

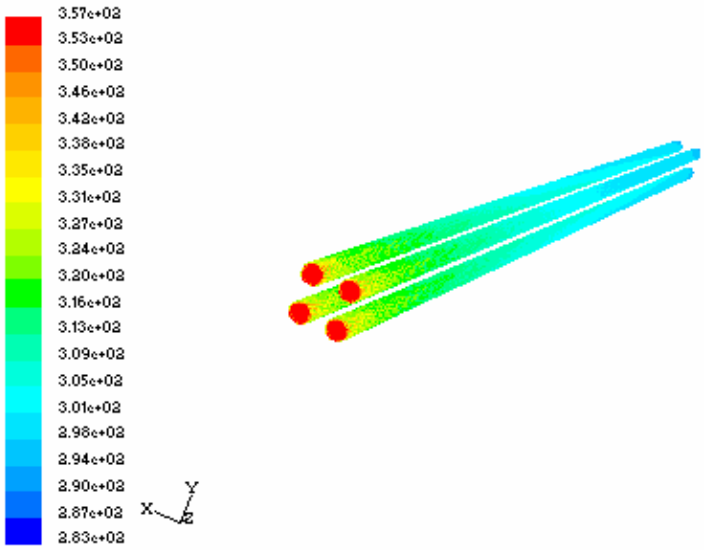

Fig: 6.13. Temperature contours for uniform mass flow distribution for square in-line tube arrangement

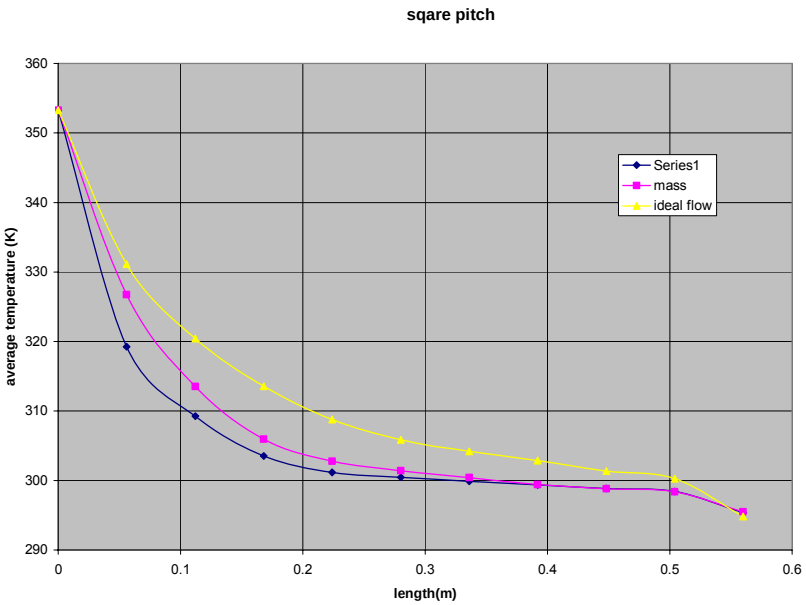

Fig: 6.14. Temperature profiles for maldistribution without back flow and uniform mass flow distribution

6.4. DISCUSSION

Single-pass shell-and-tube heat exchanger with four tube inline arrangement:

Case -1: tube side maldistribution with out back flow and shell side ideal plug flow

In this arrangement mass weighted average temperature and area weighted temperature have same value at the position $\xi=0$, Fig.6.2. The area weighted temperature profile falls below the mass weighted temperature profile along the length of the exchanger. But in the case of uniform mass flow distribution both average temperature profiles are identical along the exchanger.

Case -2: tube side maldistribution with back flow and shell side ideal plug flow:

In this arrangement area weighted temperature profile jumps below the mass weighted temperature profile at the position $\xi=0$, Fig.6.8. This is due to adiabatic mixing of the forward flow and back ward flow at the inlet bonnet. This effect reduces the effective ness of heat exchanger there by reducing the heat transfer.

6.5. Conclusion

1. It is concluded that due maldistribution without back flow on tube side and ideal plug flow on shell side, the area weighted temperature profile falls below the mass weighted temperature profile. When we compared the maldistribution with out back flow with an ideal uniform mass flow distribution, the temperature profiles of maldistribution with out back flow falls below the temperature profiles of uniform mass flow distribution.
2. Due to maldistribution with back flow on tube side and ideal plug flow on shell side, the area weighted temperature profile jumps below the mass weighted temperature profile at the beginning of the calculation domain. When we compared the maldistribution with back flow with an ideal uniform mass flow distribution, the temperature profiles of maldistribution with back flow falls much below the temperature profiles of uniform mass flow distribution.

3. Flowmaldisribution effect is similar in four tube in-line arrangement and square in-line tube arrangement for same mass flow rate and equal dimensions of the exchanger.

6.6. Scope of the future work

1. Validation of obtained temperature profiles with the numerically solved temperature profiles.
2. Validation of the fluent results with the experimental results.

Chapter 7

REFERENCES

REFERENCES

[1] Wilfried Roetzel and Chakkrit Na Ranong,. 1999, “Consideration of maldistribution in heat exchangers using the hyperbolic dispersion model” Chemical Engineering and Processing 38, pp. 675–681.

[2] Sahoo, R.K., and Wilfried Roetzel., 2002, “Hyperbolic axial dispersion model for heat exchangers” International Journal of Heat and Mass Transfer 45, pp 1261–1270.

[3] Wilfried Roetzel , Chakkrit Na Ranong., 2000 “axial dispersion model for heat exchangers” Heat and Technology vol. 18.

[4] Yimin Xuan, and Wilfried Roetzel., “Stationary and dynamic simulation of multipass shell and tube heat exchangers with the dispersion model for both fluids” Int. J. Heat Mass Transfer. Vol. 36, No. 17,4221A231,

[5] Danckwerts, P.V., 1953, Continuous flow systems Distribution of Residence times Chemical Engineering science genie chimique Vol. 2.

[6] Lalot, S., P. Florent , Langc, S.K., Bergles, A.E., 1999, “Flow maldistribution in heat exchangers “Applied Thermal Engineering 19, pp 847-863.

[7] Prabhakara Rao Bobbili, Bengt Sunden, and. Das, S.K., 2006, “An experimental investigation of the port flow maldistribution in small and large plate package heat exchangers Applied Thermal Engineering 26, pp 1919–1926.

[8] Zakro Stevanovic, Gradimir, Ilić., Nenad Radojković, Mića Vukić, Velimir Stefanović, Goran Vučković., 2001, “Design of shell and tube heat exchangers by using CFD technique- part one: thermo hydraulic calculation” Facta Universities Series: Mechanical Engineering Vol.1, No 8, pp. 1091 - 1105

[9] Wilfried roetzel and Das, S.K., 1995 “Hyperbolic axial dispersion model: concept and its application to a plate heat exchanger” Int..J. Heat Mass Transfer. Vol. 38, No. 16, pp. 3062-3076.

[10] Anindya Roy, and Das, S.K., 2001, “An analytical solution for a cyclic regenerator in the warm-up period in presence of an axially dispersive wave” Int. J. Therm. Sci. 40, pp.21–29

[11] Ping Yuan., 2003 "Effect of inlet flow maldistribution on the thermal performance of a three-fluid crossflow heat exchanger International" Journal of Heat and Mass Transfer 46, pp.3777–3787.

[12] Srihari, N., Prabhakara Rao, B., Bengt Sunden, Das, S.K., 2005 "Transient response of plate heat exchangers considering effect of flow maldistribution" International Journal of Heat and Mass Transfer 48, pp. 3231–3243.

[13] Roetzel, W., Spang, B., Luo, X., and Dash, S.K., 1998 "Propagation of the third sound wave in fluid : hypothesis and theoretical foundation" International Journal of Heat and Mass Transfer 41, pp. 2769.-2780.

[14] Zhe Zhang and YanZhong Li., 2003 "CFD simulation on inlet configuration of plate-fin heat exchangers" Cryogenics 43, pp. 673–678.

[15] Xuan, Y., and Roetzel, W., " Dynamics of shell-and-tube heat exchangers to arbitrary temperature and step flow variations" AIChE Journal Volume 39, Issue 3 , pp.413 – 421.

[16] Wilfried Roetzel, and Frank Balzereit., 2000, "Axial dispersion in shell-and-tube heat exchangers" Int. J. Therm. Sci. 39, 1028–1038.

[17] Mueller, A.C., 1987, "Effects of some types of maldistribution on the performance of heat exchangers" Heat Transfer Engineering Volume 8, Issue 2, pp. 75-86.

[18] Anil Kumar Dwivedi and Sarit Kumar Das., 2007, "Dynamics of plate heat exchangers subject to flow variations" International Journal of Heat and Mass Transfer Volume 50, Issues 13-14, pp. 2733-2743.

[19] Ranganayakulu, Ch., and Seetharamu, K.N., 2000, "The combined effects of wall longitudinal heat conduction and inlet fluid flow maldistribution in crossflow plate-fin heat exchangers Heat and Mass Transfer 36, pp. 247 ± 256.

[20] Karno, A., and Ajib, S., 2006, "Effect of tube pitch on heat transfer in shell-and-tube heat exchangers—new simulation software Heat Mass Transfer 42, pp. 263–270.